Distinct selection signatures during domestication and improvement in crops: a tale of two genes in mungbean

Ya-Ping Lin[1,2#], Hung-Wei Chen[1#], Pei-Min Yeh[1], Shashi S. Anand[1], Jiunn Lin[3], Juan Li[1,4,5], Thomas Noble[6], Ramakrishnan Nair[7], Roland Schafleitner[2], Maria Samsonova[8], Eric Bishop-von-Wettberg[8,9], Sergey Nuzhdin[10], Chau-Ti Ting[11], Robert J. Lawn[12], and Cheng-Ruei Lee[1,3]*

1. Institute of Ecology and Evolutionary Biology, National Taiwan University, Taipei 10617, Taiwan
2. World Vegetable Center Headquarter, Tainan 74199, Taiwan
3. Institute of Plant Biology, National Taiwan University, Taipei 10617, Taiwan
4. Institute of Ecology and Evolution, University of Bern, Bern, Switzerland
5. Swiss Institute for Bioinformatics, Lausanne, Switzerland
6. Queensland University of Technology, Brisbane, Australia
7. World Vegetable Center South and Central Asia, ICRISAT Campus, Patancheru, Hyderabad, Telangana 502324, India
8. Mathematical Biology and Bioinformatics Laboratory, Peter the Great St. Petersburg Polytechnic University, St. Petersburg, Russia
9. Department of Plant and Soil Science and Gund Institute for the Environment, University of Vermont, Burlington, VT 05405, USA
10. University of Southern California, Los Angeles, CA 90089, USA
11. Department of Life Science, National Taiwan University, Taipei 10617, Taiwan
12. College of Science & Engineering, James Cook University, Townsville, Queensland 4814, Australia

# Equal contribution

* *Corresponding author*
Cheng-Ruei Lee
chengrueilee@ntu.edu.tw

Keywords: *Vigna radiata*, demographic history, selective sweeps, pod shattering, stem determinacy

Abstract

Domestication and improvement are two crucial processes underlying the evolution of crops. Domestication transformed wild plants into a utilizable form for humans; improvement refined cultivars adapting to distinct environments and local preferences. Using whole-genome re-sequencing of *Vigna radiata*, we investigated the demographic history and compared the genetic footprints of domestication and improvement. The Asian wild population migrated to Australia at about 50 kya, and domestication happened in Asia about 9 kya selecting for non-shattering pods. The key candidate gene for this trait, *VrMYB26a*, has lower expression in cultivars, consistent with the reduced polymorphism in the promoter region reflecting hard selective sweep. The determinate stems were later selected as an improvement phenotype and associated with the gene *VrDet1*. Two ancient haplotypes reducing gene expression exhibit intermediate frequencies in cultivars, consistent with selection favoring independent haplotypes in soft selective sweep. Our results suggest domestication and improvement may leave different genomic signatures of selection, reflecting the fundamental differences in the two processes and highlighting the limitations of genome-scan methods relying on hard selective sweep.

Introduction

Crop evolution encompasses two phases, domestication and improvement (Hufford, et al. 2012; Li, et al. 2013; Meyer and Purugganan 2013; Abbo, et al. 2014; Giovannoni 2018; Kumar, et al. 2021). The former refers to the initiation of the divergence from the wild progenitor. Strong selection occurs upon a small population of wild progenitors, with accompanying loss of genetic and phenotypic diversity. Given that domestication aims to increase human benefits rather than plant fitness in the wild, this process typically leads to the so-called domestication syndrome, including the loss of seed shattering and dormancy, gain of gigantism, and the reduction of lateral branches. For example, teosinte (*Zea mays* ssp. *parvigalumis*), the progenitor of maize, has more lateral branches and a tendency for ear shattering than maize (Doebley, et al. 1995). *Oryza rufipogon*, the progenitor of rice, shows more easily seed shattering and smaller seeds than rice (Huang, Kurata, et al. 2012). Improvement, on the other hand, generally occurred accompanying the spread of the domesticated populations to different agro-ecological regions, primarily focusing on increasing yield and the enhanced adaptation to local environments or cultivation systems. For example, soybean varieties in northern Japan required shorter days to flowering than those in southern Japan, suggesting that the regional farmers selected soybeans according to local environments (Kaga, et al. 2012). Given the different natures of these two selection processes, it is intriguing whether they affected the underlying genes and crop genomes in different ways.

Meyer et al. (2013) proposed criteria for defining domestication and improvement genes in crops. Genes controlling domestication traits are supposed to undergo positive selection, and the causal mutations would eventually become nearly fixed in all lineages from a single domestication event (Meyer and Purugganan 2013). For example, *sh4*, the loss-of-function allele of one of the influential domestication genes controlling non-shattering in rice, is almost fixed in cultivated rice (Li, et al. 2006). On the other hand, improvement genes may exhibit different signatures of selection since the target phenotypes for improvement often differ depending on local environments and cultivation systems, diversifying the phenotypes of worldwide varieties (Huang, Zhao, et al. 2012; Zhang, et al. 2015). For instance, in soybean, the mutant allele of the flowering-time gene *E1* resulted in the change of photoperiod requirement and was enriched in specific populations,

associated with the adaptation of soybean cultivars to diverse environments (Xia, et al. 2012; Zhou, et al. 2015). Despite the general knowledge of expected differences between domestication and improvement processes, only few have specifically contrasted their genomic signatures of selection in the same species.

Vigna radiata, mungbean, a traditional legume crop in Asia, was believed to be originated in India (Purugganan and Fuller 2009). Its putative ancestor, *V. radiata* var. *sublobata*, occupies a wide range from Africa, South Asia, Indonesia, to Australia (Tateishi 1996; Castillo and Fuller 2010). Two recent studies used reduced-representation sequencing to investigate the genetic structure of cultivated mungbean (Noble, et al. 2018; Breria, et al. 2020), but genome-wide investigation comparing the cultivars and wild progenitors is lacking. The genetic architecture of trait differences between wild and cultivar groups were investigated in bi-parental crosses (Isemura, et al. 2012; Li, et al. 2018). Some of these traits are classic domesticated traits, such as the loss of pod twisting and seed dormancy, and other traits, such as plant stature and yield components, resulted from the improvement phase (Huyghe 1998; Fuller and Allaby 2018). To investigate the genomic and genetic patterns of domestication and improvement, studies using whole-genome sequencing from many wild and cultivar accessions are required.

In this study, we re-sequenced 114 *V. radiata* accessions and investigated demographic histories and origins of distinct wild and cultivar groups. We targeted two genes controlling important domestication and improvement traits, pod twisting and stem determinacy, to elucidate how artificial selections during these two processes shape genetic architecture and leave distinct selection signatures at targeted loci.

Results

Genetic variation of global *V. radiata*

The whole-genome sequencing data were generated for 114 *V. radiata* accessions (36 wild and 78 cultivars) and one accession of closely-related species, *V. mungo*. The sequencing depth was 33.52 ± 9.76X per accession. The mapping rate of these raw reads to the *V. radiata* reference genome version 6 was 98.08 ± 2.67% (Supplementary Table S1). Finally, we identified 18,548,167 (18.5 million) bi-allelic SNPs for the following analyses.

We used these SNPs to infer the genetic structure. Lower cross-validation error values of ADMIXTURE exist in K = 2 and 5 (Supplementary Fig. S1). Accessions from the same continent were clustered together when K = 2 (Figure 1A separating Asia and Australia; Supplementary Table S2). Under K = 5, the wild accessions were divided into eastern Australian ones (SubAUe), western Australian ones (SubAUw), and Asian ones (SubAS), and the cultivars were separated into two groups from South Asia (RadSA) and other regions in Asia (RadOther). A similar pattern was observed in the phylogenetic tree and network (Figure 1A-B and Supplementary Fig. S2). The mean F_{ST} value between wild and cultivar populations was 0.49, showing a high degree of differentiation. The wild groups have higher nucleotide diversity than the cultivar groups (Supplementary Fig. S3A). Likewise, LD decays much faster in the wild than in the cultivar population, reaching r^2 = 0.2 at about 22 kb and 173 kb, respectively (Supplementary Fig. S3B).

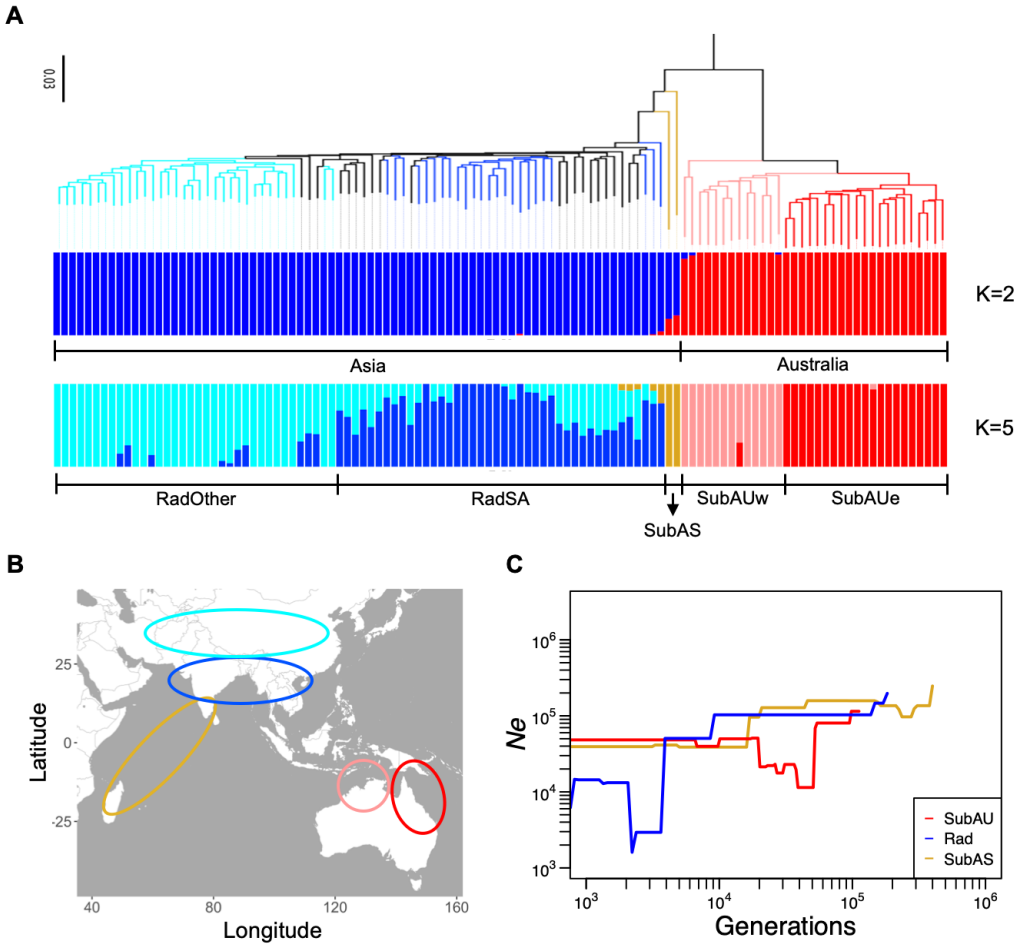

Figure 1. Population structure and demographic history. (A) Neighbor-joining phylogenetic tree and population structure of the 114 mungbean accessions. *Vigna mungo*, VI035226, is the outgroup of the phylogenetic tree. (B) Geographic distribution of the inferred genetic groups. (red: SubAUe, pink: SubAUw, goldenrod: SubAS, blue: RadSA, skyblue: RadOther) (C) Inferred demographic history.

Demographic history

Most species closely related to *V. radiata* exist in Asia (Norihiko, et al. 2010), so mungbean likely has an Asian origin. The existence of many wild accessions in Australia suggests ancient migration from Asia across the Wallace line. We estimated that the Asian and Australian groups first diverged at about 50 thousand years ago (kya) (Figure 1C, Supplementary Fig. S4A-B). After the divergence, the effective population size of SubAU decreased by about tenfold while that of SubAS remained relatively stable, consistent with SubAU being a founder population colonizing Australia. After this major vicariance between Asia and Australia, Asian cultivars (Rad) diverged from SubAS at about 9 kya (Figure 1C, Supplementary Fig. S4C). After the initial domestication, the effective population size of Rad dropped close to 20 times since 4 kya, presumably due to intensified artificial selection and coinciding with archeological records during 4 to 3 kya (Fuller 2007). The decreased effective population size of Rad might also be affected by climate change, as 4 kya coincides with the start of climate cooling after the Holocene climate optimum (Marcott, et al. 2013).

The strong divergence between Asian and Australian groups was also apparent from the 2D site frequency spectrum comparing Rad, SubAUe, and SubAUw (Supplementary Fig. S5). SubAUe and SubAUw had more shared four-fold degenerate SNPs than each of them with Rad, consistent with their closer relationship. On the contrary, SNPs with high impact were enriched in low-frequency derived-allele categories with few shared between populations. These SNP sites were probably under negative selection, and presumably, detrimental ancestral variations were unlikely to be retained in both descendant populations.

Our results suggested Austalian wild (SubAU) population diverged from the Asian wild group (50 kya) (Figure 1C) during the last ice age (115-11.7 kya), which allows us to track the change in the environmental niche space of these groups. During the last interglacial

period (120-140 kya), when *V. radiata* had not colonized Australia, Australia was a less suitable habitat for the Asian groups (Figure 2). During the last ice age, the Sunda Shelf and northern Sahul Shelf were suitable for both the Southeast Asia and Southern Hemisphere populations, facilitating the expansion of *V. radiata* from Southeast Asia into Australia both geographically and environmentally (Figure 2, Supplementary Fig. S6). The Schoner's D values (higher values representing higher niche similarity) also supported that the Southern Hemisphere population shared more suitable habits with the Southeast Asian population (0.612) than the South Asian one (0.418). At present, most of the Malay Archipelago and Australia appear unsuitable for the South and Southeast Asia populations. However, continental Southeast Asia and northern Australia appear suitable for the Southern Hemisphere population.

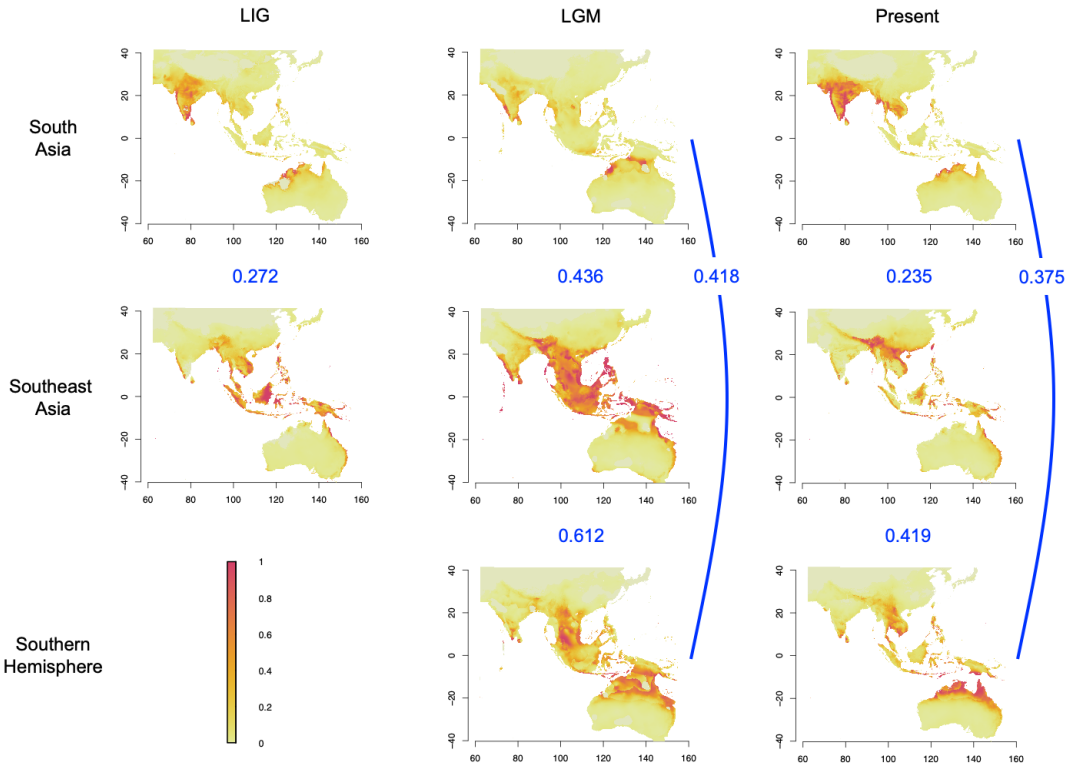

Figure 2. Ecological niche modeling of suitable habitats for the wild mungbean populations in South Asia, Southeast Asia, and Southern Hemisphere from the past to present. Colors represent niche suitability. The three rows (South Asia, Southeast Asia, and Southern Hemisphere) represent niche models constructed from the presence data of wild mungbean from these regions and projected to the whole geographical extent. Data of

Last Interglacial period (120-140 kya, LIG) and the Last Glacial Maximum (22 kya, LGM) were based on the circulation model of MIROC-ESM. The numbers in blue between pairs of modeled distribution indicate the Schoner'D values, where higher values represent higher niche similarity.

Selective sweeps in mungbean

We used three approaches to investigate selection footprints across the genome. Potentially selective signals across the genomes of wild and domesticated mungbeans were detected by identifying the regions with the top 1% value in the composite likelihood ratio (CLR) analysis (Figure 3A-B). There were 429 genes detected across the wild genome, and the gene ontology (GO) analysis showed that these genes were significantly enriched in the function of the protein binding and metabolic process (Supplementary Fig. S7A). Comparing our selection scan results to previous QTL mapping explicitly focusing on the divergence between wild and cultivar accessions (Isemura, et al. 2012), the wild accessions' alleles of these QTL generally have more pods, a higher proportion of shattering pods, and smaller seed size.

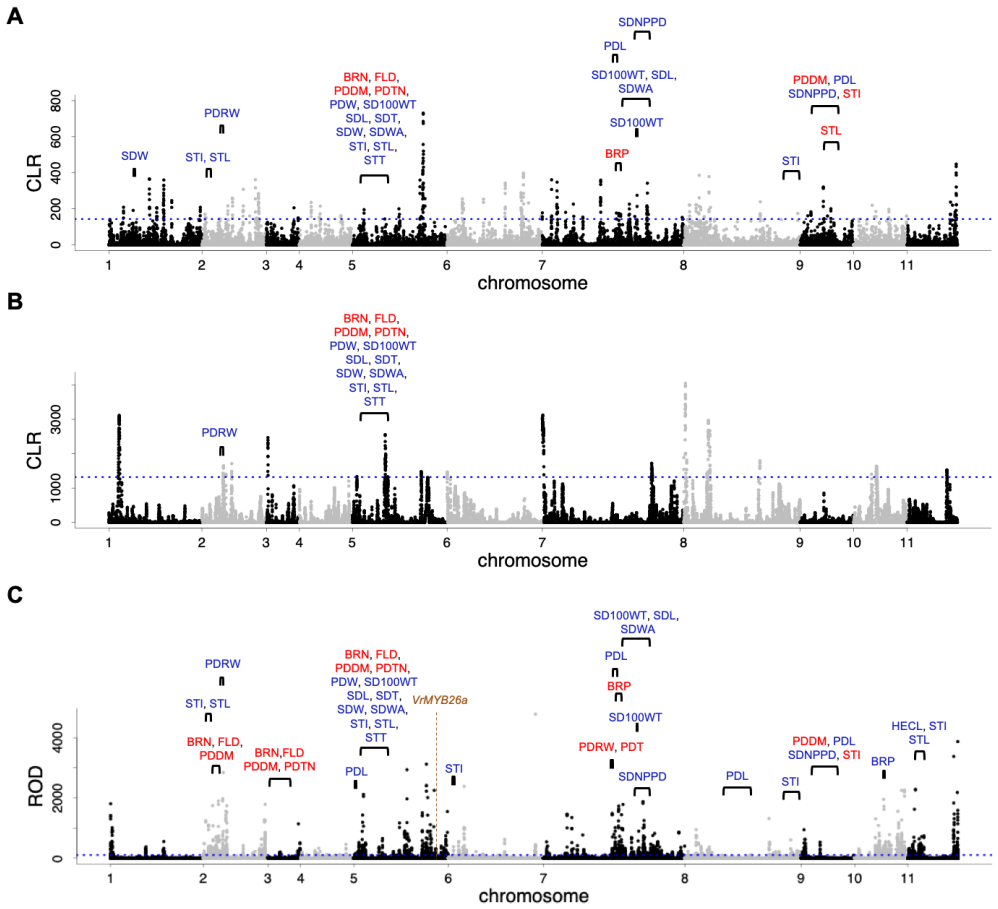

Figure 3. Signatures of selection across the mungbean genome. Composite likelihood ratio (CLR) values across the genomes of the (A) wild and (B) domesticated mungbean. (C) Selective sweeps during domestication inferred from reduction of diversity (ROD) values. To improve the accuracy, only the QTL with the interval < 15 Mb and overlapped with selection signals were labeled. The red and blue texts indicate wild or cultivar alleles have higher trait values in the QTL, respectively. The blue horizontal dashed lines indicate the cut-off (top 1%) of candidate selective signals. One of the candidate domestication genes, *VrMYB26a*, was labeled with brown color. (Abbreviation of traits- BRN: branch number, BRP: position of the first branch, FLD: days to first flower, HECL: hypocotyl plus epicotyl length, PDDM: days to maturity of the first pod, PDL: pod length, PDRW: rate of shattered pods, PDT: number of twist of the shattered pod, PDTN: total pod number, PDW: pod width, SD100WT: 100 seed-weight, SDL: seed length, SDNPPD: number of seeds per pod, SDT: seed thickness, SDW: seed width, SDWA: seed water absorption, STI: stem internode length, STL: stem length, STT: stem thickness).

For cultivated mungbean, the selected regions across the cultivar genome colocalized with the QTL where the cultivar alleles conferred lower pod dehiscence and fewer pods.

There were 420 candidate genes in selected regions, and the GO terms were enriched in carbohydrate binding, response to biotic stimulus, and regulation of nitrogen compound metabolic process (Supplementary Fig. S7B). Notably, legumes are able to form a symbiotic relationship with rhizobia, a unique characteristic involving in nitrogen fixation process(Janczarek, et al. 2015). Thus, enrichment results suggested the important role of mungbean cultivars for soil fertility. This is supported by the first written record of mungbean in an ancient Chinese agricultural literature (齊民要術, Qimin Yaoshu, 544 AD), which emphasized its value as green manure. Other ancient Chinese sources also repeatedly mentioned using mungbean to restore soil fertility in the rotation system (Chen 1980).

A total of 1,232 genes have potential signatures of selective sweeps from the reduction of diversity (ROD) method comparing cultivars relative to wild accessions (Figure 3C). These candidate genes were enriched in GO terms such as catalytic activity, DNA binding, developmental growth, and response to stimulus and chemicals (Supplementary Fig. S7C). Among them, *INVA* is one of the candidate genes responsible for seed size in durum wheat (Mangini, et al. 2021). *ARG1* is the ortholog of the omega-3 fatty acid desaturase gene (*FAD3*), which influences the oil composition in soybean seeds (Bilyeu, et al. 2005; Pham, et al. 2012). *BG7S-2* is likely responsible for basic 7S globulin, one of the storage proteins in mungbean seeds (Mendoza, et al. 2001; Hirano 2021). The high-ROD regions colocalized with the QTL regulating phenology, pod and seed enlargement, pod twisting and dehiscence, and yield. Overall, these results suggested that the wild mungbean was likely under natural selection for dispersal: the wild alleles of these QTL generally have more pods, a higher proportion of shattering pods, and smaller seed size. On the other hand, the cultivars were selected for pod non-shattering as well as pod and seed gigantism, with fewer pods as a potential trade-off.

VrMYB26a associated with the domestication trait pod non-shattering

In legumes, loss of pod twisting is one of the essential traits during domestication (Fuller and Allaby 2018). Among all the putative domestication genes, *MYB26*, which is involved in pod shattering in *Phaseolus vulgaris*, *Vigna angularis*, and *V. unguiculata* (Takahashi, et al. 2020; Di Vittori, et al. 2021), was detected to be under positive selection in the cultivars (Figure 3C). The thickness of the lignified sclerenchyma layer on the pod walls

243 strongly correlates with the coiling of pod walls (Takahashi, et al. 2020; Parker, et al. 2021).
244 Like other legume species, mungbean cultivars have a thinner lignified layer than wild
245 accessions (Figure 4A). Mungbean has two *MYB26* copies, one on chromosome 5
246 (*VrMYB26a*) and the other on chromosome 9 (*VrMYB26b*). According to the phylogenetic
247 relationship with the other legume homologs, *VrMYB26a* was clustered with the *MYB26*
248 orthologs associated with pod shattering in *P. vulgaris*, *V. angularis*, and *V. unguiculata*
249 (Clade A), and the other clade contained *VrMYB26b* (Clade B) (Supplementary Fig. S8A).
250 The genes in Clade A showed lower d_N/d_S than those in Clade B (Supplementary Fig. S8B),
251 indicating a stronger selection constraint in the former clade. Despite larger difference of
252 allele frequency of three non-synonymous SNPs between wild and cultivars in *VrMYB26a*
253 coding region, the function of its encoding protein is probably not changed due to the
254 similar property of amino acids. (Supplementary Fig. S9). We inferred whether the
255 differential expression, instead of amino acid changes, results in non-twisting pods in
256 cultivars.
257

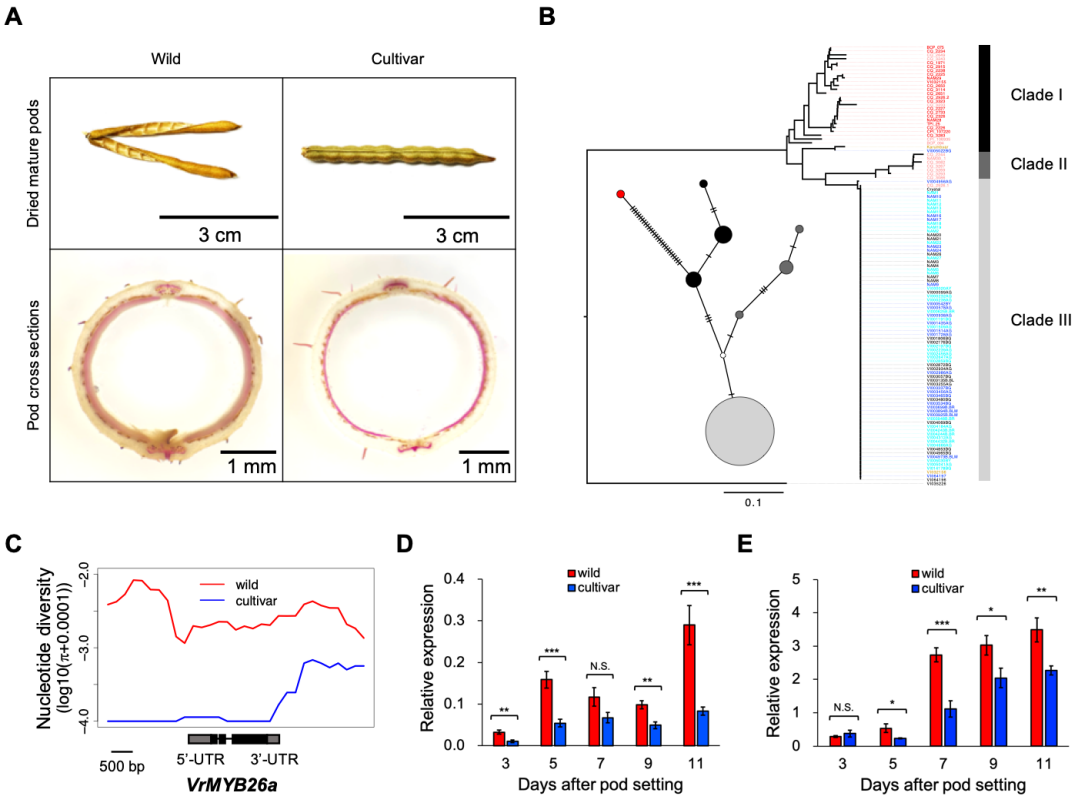

Figure 4. *VrMYB26a* associated with pod twisting in mungbean. (A) Mature pods and pod cross-sections from the wild (NAM30) and cultivated (VI004853) mungbean accessions. The cross-section's lignin was stained in red. (B) Neighbor-joining tree of *VrMYB26a* promoter region (upstream 2kb) of 114 mungbean accessions and one *V. mungo* as outgroup. Accession names are labeled with colors based on population structure (K = 5). Also shown is the haplotype network based on 61 SNPs in the same region, and the outgroup was labeled with a red dot. Haplotypes were colored based on the clades identified from the tree. The sizes of circles correspond to the number of individuals in this haplotype. (C) Patterns of nucleotide diversity in sliding windows (window size, 1 kb; step size, 0.2 kb) of the wild and cultivar groups from the 2-kb upstream of *VrMYB26a* to its 2-kb downstream regions. (D) Expression levels of *VrMYB26a* during pod development. (E) Expression levels of *VrCAD4* during pod development. In (D) and (E), three accessions of wild and cultivar groups were used, respectively. The data are presented as mean ± standard error (N.S. indicates non-significant; *, **, and *** indicate p value < 0.05, 0.01 and 0.001, respectively).

The neighbor-joining tree and haplotype network of the *VrMYB26a* promoter region (upstream 2kb) supported the near-fixation of the derived allele in cultivars (Figure 4B). Together with the apparent reduction of nucleotide diversity at the upstream of *VrMYB26a*

in cultivars (Figure 4C), these lines of evidence suggested that the expression pattern of *VrMYB26a* was the likely target of selection for non-twisting pods. We then evaluated the gene expression of *VrMYB26a* during pod development. The wild accessions showed significantly higher expression of *VrMYB26a* than cultivars on average, except on the 7th day after pod setting (DAP) (Figure 4D). Similarly, the expression of *VrCAD4*, a critical downstream gene involved in lignin biosynthesis (Xie, et al. 2018), was significantly higher in wild accessions than cultivars, except on the 3th DAP (Figure 4E). This suggested the lower expression of *VrMYB26a* reduced expression of downstream lignin biosynthesis gene, which contributed to non-twisting pods with thinner sclerenchyma layer. The gene responsible for pod non-shattering, an important trait in mungbean domestication, likely experienced the classic pattern of a hard selective sweep, where most cultivars share the same derived allele with low variation.

***VrDet1* associated with the improvement trait stem determinacy**

Plant architecture, associated with seed yield and environmental adaptation, is often the target of artificial selection during the improvement phase (Huyghe 1998). Like other legume species, wild mungbeans have indeterminate growth, while many cultivars have determinate growth (Nguyen, et al. 2012; Chauhan and Williams 2018), an improved phenotype advantageous for harvesting due to the shorter reproductive periods (Nair, et al. 2020). A previous study has shown that *VrDet1* modulated determinacy (Li, et al. 2018). The phenotypic shift from indeterminate to determinate growth was caused by two single nucleotide substitutions at the -1058 and -14 sites upstream of *VrDet1*, reducing its expression. While the previous study was based on only a few wild and cultivar accessions, our comprehensive sampling identified several cultivars with the indeterminate phenotype (Figure 5A). Thus, we further investigate patterns of polymorphism in this essential gene.

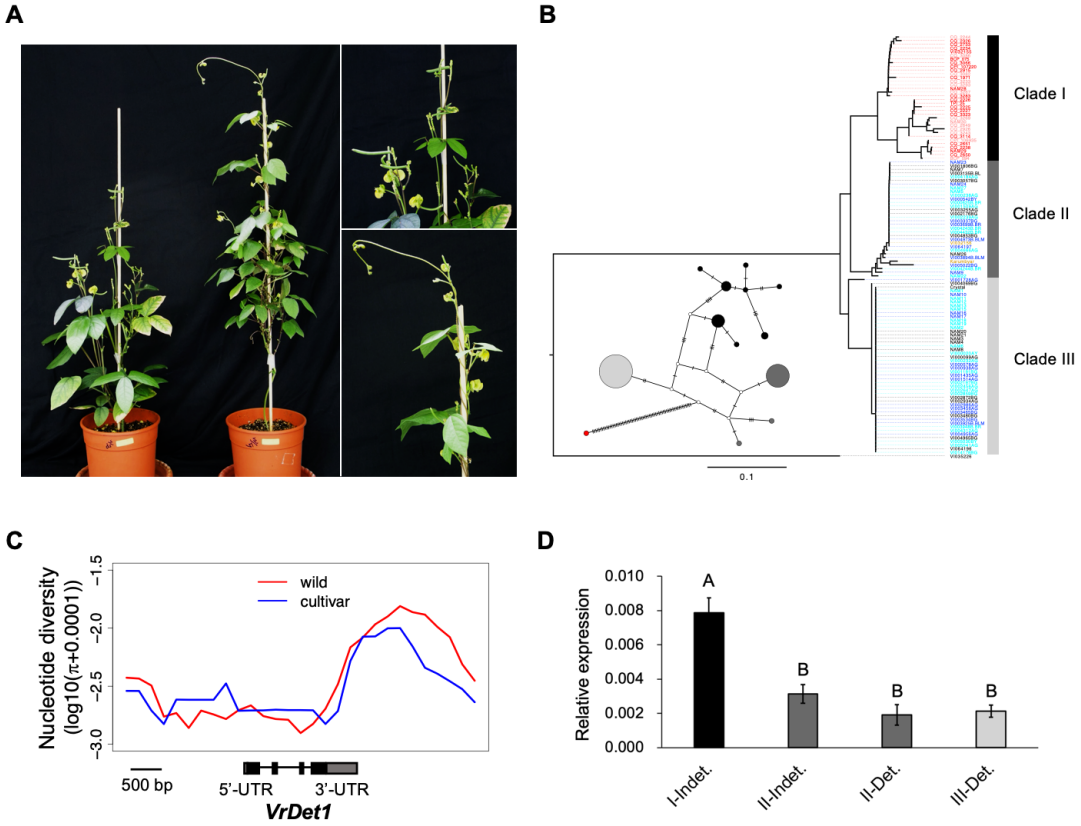

Figure 5. Stem determinacy and its relationship with *VrDet1*. (A) Left: Photographs of indeterminate and determinate mungbean accessions at the reproductive stage. Upper right: the enlargement of terminal flowers and pods at the main apical stem in a determinate accession. Lower right: the enlargement vegetative growth at the main apical stem in an indeterminate accession. (B) Neighbor-joining tree of the *VrDet1* promoter region (upstream 2kb) of 114 mungbean accessions and one *V. mungo* as an outgroup. Accession names are labeled with colors based on population structure (K = 5). Also shown is the haplotype network based on 85 SNPs in the same region, and the outgroup was labeled with a red dot. Haplotypes were colored based on the clades identified from the tree. The sizes of circles correspond to the number of individuals in this haplotype. (C) Patterns of nucleotide diversity in sliding windows (window size, 1 kb; step size, 0.2 kb) of the wild and cultivar groups from the 2-kb upstream of *VrDet1* to its 2-kb downstream regions. (D) Expression levels of *VrDet1* in the four groups. Colors represent the clades in (B). The data are presented as mean ± standard error ($p < 0.001$. Different letters indicate significant differences from Tukey's HSD-test).

Non-synonymous SNPs were not found in the *VrDet1* coding region among cultivars, suggesting that the polymorphism of determinacy in cultivars was not associated with

amino acid changes in this gene (Supplementary Fig. S10). The only two non-synonymous SNPs across all of our samples also have low allele frequency differences between cultivar and wild accessions (Supplementary Fig. S10). The neighbor-joining tree of the putative promoter region of *VrDet1* (upstream 2 kb) showed three distinct clades. All Australian wild (SubAU) accessions were clustered in Clade I, two Asian wild (SubAS) accessions clustered in Clade II, and the cultivars clustered in Clade II and III (Figure 5B). The haplotype of the two causal SNPs in Clade I was T^{-14}/T^{-1058}, and that in Clade III was A^{-14}/C^{-1058}, respectively corresponding to the typical wild and cultivar forms observed in the previous study (Li, et al. 2018). Interestingly, Clade II represents a novel haplotype, T^{-14}/C^{-1058}, with the first site corresponding to the wild but the second corresponding to the cultivar alleles. Among accessions with the Clade II haplotype, the two SubAS accessions and eight cultivars were indeterminate, and 22 out of 30 cultivars showed determinate growth. Almost all cultivars in Clade III showed determinate growth.

To test whether Clade II (T^{-14}/C^{-1058}) originated from a recent recombination event between the wild Clade I (T^{-14}/T^{-1058}) and the "typical cultivar" Clade III (A^{-14}/C^{-1058}) haplotypes, in this upstream 2 kb region we identified nine diagnostic SNPs with high allele frequency differences between Clade I and III. We used these SNP sites to polarize the allele frequencies in the newly identified Clade II. Instead of the typical patterns of recent recombinant haplotype, where one side of the Clade-II haplotype would conform to Clade-I and the other correspond to Clade-III major alleles, the allele frequencies of Clade II zigzagged among these SNPs (Supplementary Fig. S11). This suggests that Clade II (T^{-14}/C^{-1058}) is an ancient haplotype, which is also supported by the haplotype network where haplotypes in both Clade II and Clade III are closer to the root (Figure 5B). Since the cultivars contained two haplogroups of intermediate frequencies, no obvious lack of variation was observed in cultivars compared to wild accessions (Figure 5C). On the other hand, many accessions within Clade II or Clade III possess identical sequences, suggesting their independent rapid frequency increase (Figure 5B).

The gene expression level of *VrDet1* in Clade II and III was significantly lower than that in Clade I (Figure 5D), consistent with their determinate phenotype. Notably, the indeterminate accessions in Clade II did not show significantly higher expression than the determinate accessions in Clade II or Clade III, suggesting *VrDet1* expression might not be

the only factor affecting stem determinacy. The results suggested that Clade II (T^{-14}/C^{-1058}) may have weaker effects than Clade III (A^{-14}/C^{-1058}) and have incomplete penetrance, sometimes allowing other genes to cause the ancestral indeterminate phenotype. This is consistent with Clade II containing one wild (T^{-14}) and one cultivar (C^{-1058}) allele in the two SNPs previously shown to affect gene expression (Li, et al. 2018).

Taken together, our results suggested that the evolution of the improvement trait, stem determinacy, appears to be more complex than the previously suggested simple model of hard selective sweep from the "typical cultivar" Clade III haplotype (Li, et al. 2018). Instead, the evolution might result from soft sweeps of two ancient haplotypes (Clade II T^{-14}/C^{-1058} and Clade III A^{-14}/C^{-1058}) reducing the expression of *VrDet1*, with Clade II showing incomplete penetrance allowing the indeterminate phenotype under certain environmental or genomic contexts.

Discussion

In this study, we used whole-genome sequencing to investigate the history of *Vigna radiata* before, during, and after domestication. Our results suggest *Vigna radiata* originated in Asia, and the wild population of Southeast Asia likely migrated to Australia during the last ice age. This is supported by the geographical proximity and niche similarity between Southeast Asia and Australia. Domestication probably happened at 9 kya in Asia, after which the cultivars had high selection pressure during domestication for loss of pod shattering to prevent yield loss. Subsequently, some cultivars with determinate shoot growth were selected during improvement. Given the different nature of selection during the domestication and improvement phases, we showed that the candidate genes for these two traits exhibit distinct signatures of selection.

The evolution of *V. radiata*

We proposed a hypothesis of the evolution of *V. radiata*: wild mungbean originated in Asia and migrated into Australia at about 50 kya. This coincides with the initial occupation of Australia by humans (Tobler, et al. 2017), and interestingly, it has been recorded that the tuberous roots of wild mungbean were consumed by Aboriginal Australians (Lawn, et al. 1988). Whether the immigrations of mungbean and human into Australia are associated

remains to be further investigated. Compared to their Asian counterparts, wild Australian mungbean evolved smaller seeds (Supplementary Table S3) (Lawn and Rebetzke 2006), likely as an adaptive strategy for dispersal. While wild populations both have twisting pods, the domestication starting at about 9kya further selected for pod non-twisting (Figure 6). Traditional mungbean cultivars were indeterminate (Nair, et al. 2020), and determinate cultivars were further selected during improvement. The phenomenon of two-step artificial selection also occurred in other crops. For example, in rice, seed dormancy and seed shattering were under artificial selection during domestication, while plant height and flowering time were modified locally during improvement (Liu, et al. 2018). The two-step selection in similar traits also occurred in wheat (Roucou, et al. 2018). In tomatoes, yield-related traits were first selected during domestication, and traits of flavor and color were selected in cultivars during improvement (Schouten, et al. 2019).

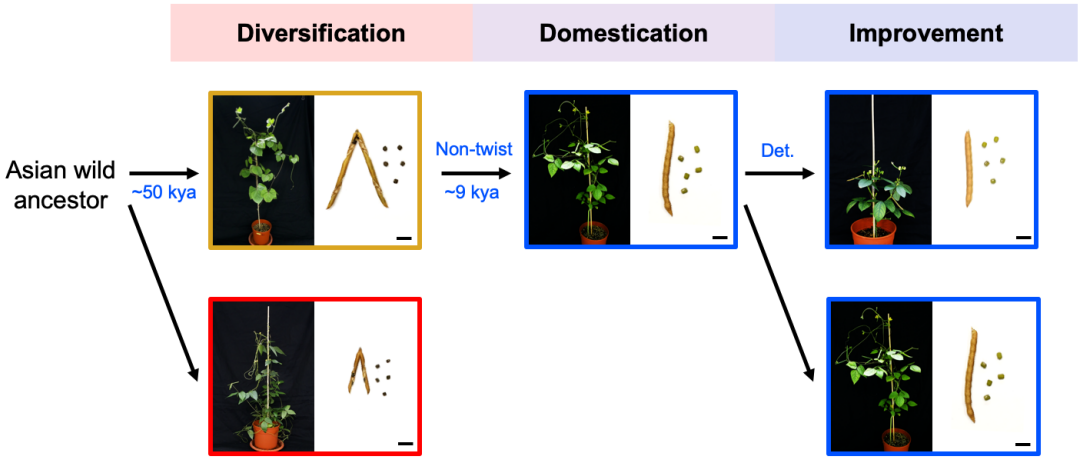

Figure 6. The hypothesis of mungbean evolution. A wild progenitor of *V. radiata* experienced species diversification, resulting in the divergence of *V. radiata* var. *sublobata* into SubAS (goldenrod box) and SubAU (red box) in about 50 kya. SubAS was further selected for pod non-twisting, becoming *V. radiata* var. *radiata* (blue boxes) during domestication (about 9 kya). Afterwards, some indeterminate cultivars are improved into determinate forms. Bar = 1 cm.

Different selection forces resulting in distinct patterns of genetic variation

In legumes, mutations of genes for pod shattering reduce the torsion of pod walls or strengthen the sutures, contributing to non-shattering pods (Parker, et al. 2021). Our result

showed that the lower expression of *VrMYB26a* in mungbean cultivars is associated with the thinner sclerenchyma layer in non-twisting pods. In *Vigna angularis* and *V. unguiculata,* it has been shown that mutations creating truncated protein of *MYB26* are likely responsible for non-twisting pods in cultivars (Takahashi, et al. 2020). In *Phaseolus vulgaris*, down-regulation of *PvMYB26* contributed to indehiscent pods (Di Vittori, et al. 2021). These findings reflects Vavilov's Law of Homologous Series in Variation, which stated that parallel evolution in closely-related species often involve genetic changes in homologous genes due to their conserved functions (Vavilov 1922, 1951). In addition, although archeological evidences suggested two possible domestication origins of mungbean from northern and southern India (Fuller and Harvey 2006), only one haplotype was observed in *VrMYB26a* promoter region across all cultivars. We suggested that mungbean likely went through only one domestication event for non-twisting pods. Consistent with the general trend in domestication genes under strong directional selection, we found evidences of hard selective sweep in *VrMYB26a.*

As for stem determinacy, indeterminate and determinate growth widely exists in cultivars (Eshed and Lippman 2019). Indeterminate crops have relatively high yields because they provide extended harvest periods and unconstrained canopy development (Chauhan and Williams 2018). Determinate types have short plant height, lodging resistance, and uniform maturity properties (Lawn 1989; Kato, et al. 2019). These two growth habits have different performances under different climate regions or agricultural practices. In the northern regions of America and China, indeterminate soybean varieties are commonly used due to their greater yield under lower temperatures and limited rainfall (Specht, et al. 2014; Kato, et al. 2015; Liu, et al. 2015). In contrast, determinate varieties dominate southern regions (Kilgore-Norquest and Sneller 2000). In mungbean, subsistence farmers prefer cultivating indeterminate varieties for multiple harvesting (Hewavitharane, et al. 2010; Depenbusch, et al. 2021), whereas determinate varieties were commonly used in intensive farming (Nair, et al. 2020). These two types of mungbean cultivars have existed in China since at least the 16th century, as recorded in The Compendium of Materia Medica (本草綱目 Ben Cao Gang Mu, 1578 AD) (Li 2016) and Chinese encyclopedia of technology (天工開物 Tian Gong Kai Wu, 1637 AD) (Song, et al. 1997). The previous

study identified alleles (A^{-14} and C^{-1058}) in two SNPs of *VrDet1* responsible for determinate growth in mungbean (Li, et al. 2018). We found that two ancient haplotypes (Clade II T^{-14}/C^{-1058} and Clade III A^{-14}/C^{-1058}) reduced *VrDet1* expression, suggesting these two haplotypes were selected when determinate varieties were preferred during improvement and consistent with soft selective sweeps (Garud, et al. 2015; Harris, et al. 2018). In soybean, multiple haplotypes of *GmTFL1* associated with determinate growth in soybean were also observed (Liu, et al. 2015). In the cross between two accessions with Clade I and Clade III haplotypes, Li et al. showed perfect co-segregation between determinacy traits and SNP markers in the promoter region (Li, et al. 2018). This suggests the complete penetrance and strong effect of Clade III (A^{-14}/C^{-1058}). It's worth noting that some cultivars with Clade II haplotype (T^{-14}/C^{-1058}) displayed an indeterminate growth, suggesting this haplotype may have incomplete penetrance allowing the generation of indeterminate phenotype under specific environmental or genomic contexts (Pierce 2012). Under specific environments or agricultural practices where the indeterminate phenotype was preferred, the Clade II haplotype may be favored. In brief, our results showed that multiple adaptive haplotypes of *VrDet1* were selected in mungbean cultivars, resulting in a pattern distinct from the typical signatures of hard selective sweep.

Conclusion

In this work, we investigated the evolutionary history of *Vigna radiata* using genomic approaches. Our comparison of phylogenetic tree, haplotype network, and signature of selection at *VrMYB26a and VrDet1* loci elucidated distinct genetic architecture behind different phases of artificial selection. For a trait and the relevant gene under selection during the domestication phase, pod twisting and *VrMYB26a* in our case, a hard selective sweep was detected with the near-complete fixation of one derived haplotype in cultivars. For a trait and the relevant gene during the improvement phase, determinacy and *VrDet1* in our case, phenotypic polymorphisms and genetically diverse haplotypes at the locus were observed in cultivars. With whole-genome resequencing of diverse wild and cultivars, we clarify the demographic history of mungbean and revealed distinct patterns of genes affected by artificial selection during crop domestication and improvement phases.

Materials and Methods

Plant materials, library construction, and sequencing

114 *V. radiata* accessions and an outgroup, *V. mungo*, were obtained from two genebanks: the World Vegetable Center in Taiwan and the Australian Grains Genebank (AGG). The passport data from the genebanks provided the taxonomy and country of origin for each accession (Supplementary Table S2). The genomic DNA was extracted from leaves with the DNeasy Plant Mini Kit (QIAGEN). DNA libraries were constructed using NEBNext® Ultra™ II DNA Library Prep Kit for Illumina (E7645), and 150-bp paired-end sequencing was completed using Illumina Hiseq X Ten.

Variant calling

Raw sequencing reads were trimmed with SolexaQA++ v3.1.7.1 (Cox, et al. 2010). Then adaptor sequences were removed with cutadapt v1.14 (Martin 2011). The cleaned reads were mapped to the mungbean cultivar (VC1973A) reference genome version 6 (Vradiata_ver6) (Kang, et al. 2014) with Burrows-Wheeler aligner v0.7.15 (Li and Durbin 2009). Duplicated reads were marked with Picard v2.9.0-1 (http://broadinstitute.github.io/picard/). Single-nucleotide polymorphisms (SNPs) were called with GATK v3.7 following the GATK Best Practice (McKenna, et al. 2010; Van der Auwera, et al. 2013). We used vcftools v0.1.13 (Danecek, et al. 2011) with following parameters "--min-alleles 2 --max-alleles 2 --remove-indels --max-missing 0.9 --minQ 30" to filter and retain bi-allelic SNPs. For LD decay and fixation index (F_{ST}) analyses, SNPs with minor allele frequency (MAF) < 0.05 were further removed.

Gene prediction and annotation

Given that the public gene annotation of *V. radiata* contains only 29,006 genes, which are much less than closely related species (Kang, et al. 2014), we re-annotated the reference genome comprehensively. The whole Vradiata_ver6 genome without masking repeats was annotated ab initio with Augustus v3.3.2 using -species Arabidopsis option (Stanke, et al. 2006). For RNAseq evidence, we downloaded RNA sequencing reads from seeds, pods, flowers, and one-week-old and four-week-old whole plants (Chen, et al. 2015; Liu, et al. 2016). These RNA reads were mapped onto the Vradiata_ver6 genome with HISAT v2.1.0

(Kim, et al. 2015) and assembled and merged by StringTie v1.3.5 (Pertea, et al. 2015). We then blasted the assembled transcripts using blastp v2.8.2 (Camacho, et al. 2009) on the UniProt database (https://www.uniprot.org/) and predicted Open Reading Frames using TransDecoder v5.5.0 (Haas, et al. 2013). For protein evidence, the *Glycine max* protein sequences (Wm82.a2.v1) (https://soybase.org/) were used as reference protein evidence and aligned to the Vradiata_ver6 genome with exonerate v2.4(Slater and Birney 2005). All these evidences were submitted to Evidencemodeler v1.1.1 (Haas, et al. 2008) to identify consensus gene models. The weight of evidence was five except for ab initio evidence, which was one. Finally, the consensus gene models were blasted in the databases of TRAPID (http://bioinformatics.psb.ugent.be/trapid_02/), eggNOG-mapper (Huerta-Cepas, et al. 2017), and plaza (Van Bel, et al. 2018) for functional annotation.

Niche modeling

We used the occurrence data of *V. radiata* var. *sublobata* based on the Global Biodiversity Information Facility (GBIF; https://www.gbif.org/) and also the collection sites of the wild samples from the Australian Grains Genebank (AGG) and National Bureau of Plant Genetic Resources (NBPGR) to identify the niche of the wild mungbean. The species distribution ranged from 32.927146° N, 66.501760° E to 27.820616° S, 155.770869° E. To avoid the over-represented occurrence in a single geographic grid, we removed the overlapped occurrence in the combined data, resulting in 22, 26, and 39 samples in South Asia, Southeast Asia, and Southern Hemisphere, respectively (Supplementary Table S4). Nineteen bioclimatic variables, including the current data (1960-1990) and the paleoclimatic data, were downloaded in the highest resolution from WorldClim 1.4 version (https://www.worldclim.org/data/v1.4/worldclim14.html). The paleoclimatic data refers to the periods of the Last Glacial Maximum (LGM: 22,000 years ago) under the MIROC-ESM and CCSM4 models, and the Last interglacial (LIG: 120,000-140,000 years ago) under the MIROC-ESM model. After removing the highly correlated bioclimatic variables (Pearson's correlation), we kept six bioclimatic variables in the niche modeling, including BIO1, BIO2, BIO3, BIO12, BIO15, and BIO18, after removing the highly correlated bioclimatic variables (Pearson's correlation coefficients > 0.8). The niche

528 modeling and projection were performed with MaxEnt v3.4.3 using default settings
529 (Phillips, et al. 2006).
530
531 **Population genomics**
532 We inferred population structure with ADMIXTURE v1.3 (Alexander, et al. 2009). An
533 accession was defined as admixed if none of its single ancestral components was more than
534 0.7. The neighbor-joining tree was constructed with TASSEL v5.0 (Bradbury, et al. 2007)
535 and plotted with Figtree v1.4.4 (http://tree.bio.ed.ac.uk/software/figtree/). Nucleotide
536 diversity (π) and fixation index (F_{ST}) were calculated using vcftools v0.1.13 (Danecek, et
537 al. 2011). Linkage disequilibrium (LD) between SNPs was calculated with PopLDdecay
538 v3.41 (Zhang, et al. 2019). To examine the relationship among populations, we estimated
539 the genetic distance of 115 accessions with a bi-allelic SNP dataset using Plink v1.90b4.5
540 (--distance) (Purcell, et al. 2007) and then constructed a phylogenetic network with the
541 neighbor-net algorithm in SplitsTree v5.3 (Huson and Bryant 2006).
542
543 **Demographic history**
544 We reconstructed the demographic history of *V. radiata* with SMC++ v1.15.2 (Terhorst,
545 et al. 2017) since this algorithm accepts many samples for a population. Since such an
546 algorithm treats two gene copies within a diploid individual as two randomly sampled
547 haplotypes from the populations and *V. radiata* is a self-fertilizing species, we followed
548 common practices for species like *Arabidopsis thaliana* and soybean (Alonso-Blanco, et
549 al. 2016; Kim, et al. 2021). We generated artificial diploids by assembling haplotypes from
550 two random accessions, except for the admixed accessions, including two wild accessions
551 (NAM30, CPI_106935) and one cultivar (VI005022BG). In addition, the heterochromatic
552 regions, which were defined by regions enriched in repetitive sequences in the
553 Vradiata_ver6 genome, were excluded. We estimated the divergence time among
554 cultivated *V. radiata* var. *radiata*, the wild group from Australia (SubAU), and the wild
555 group from Asia (SubAS), assuming one generation per year with a mutation rate at 1×10^{-8}
556 (von Wettberg, et al. 2018). We annotated potential effects of SNPs with SnpEff v4.3t
557 (Cingolani, et al. 2012), and SNPs annotated as high or low impacts were used to generate
558 unfolded 2D Site Frequency Spectrum (2D SFS) using *V. mungo* as the outgroup.

559

560 **Detection of selective sweeps**

561 Admixed accessions between wild and cultivar groups were removed from the analyses
562 of selection signals during domestication. Reduction of diversity (ROD; $\pi_{wild}/\pi_{cultivar}$) was
563 calculated in 10-kb windows with a 1-kb step size. A composite likelihood ratio (CLR) test
564 was performed with SweeD v4.0.0 (Pavlidis, et al. 2013) in non-overlapping 10-kb sliding
565 windows across the genome. Quantitative trait loci (QTL) of the domestication traits were
566 detected based on previous research (Isemura, et al. 2012) by anchoring their linked
567 markers to the reference genome. Gene ontology (GO) enrichment of the genes under
568 selection was estimated using TBtools v1.098 (Chen, et al. 2020).

569

570 **Phenotyping**

571 The mungbean plants were grown in a growth chamber under 12 hours (30°C) light/ 12
572 hours (25°C) dark at 700 μmol m^{-2} s^{-1} of light. For stem determinacy, accession was
573 defined as determinate when apical meristems stopped growing soon after flowering. For
574 pod twisting, pods from wild and cultivar accessions were dried in an oven at 37°C for four
575 days before phenotyping. The weight of 100 seeds was the average of three plants in each
576 accession. The number of seeds per pod and pod length was the average of 30 pods (10
577 pods per plant, a total of 3 plants) of each accession.

578 The sclerenchyma tissues, which contain the lignified cell walls, were observed with
579 phloroglucinol–HCl solution (Pomar, et al. 2002). We collected fresh mature pods for
580 histological staining. The phloroglucinol–HCl solution was prepared by dissolving 0.2 g
581 phloroglucinol in 20 ml ethanol and additional 20 ml 37% hydrochloric acid. The free-hand
582 cross-sections of pods were obtained with a razor blade (Corrux) and incubated in
583 phloroglucinol–HCl solution for one minute. We observed the stained slides under an
584 optical dissecting microscope (SZ61; Olympus).

585

586 **RNA isolation and real-time qPCR for *MYB26* and *VrDet1***

587 To detect *MYB26* gene expression during pod development, we collected pods 3, 5, 7,
588 9, and 11 days after pod setting (DAP). Seeds were manually removed except pods at 3 and
589 5 DAP (seeds were too small). A total of 50 mg pod tissues per sample were ground with

liquid nitrogen in a 1.5-ml microcentrifuge tube and treated with 65 °C 1.2 ml CTAB buffer (2% CTAB, 1% polyvinylpyrrolidone 40, 2 M sodium chloride, 100 mM Tris-HCl, 20 mM ethylenediaminetetraacetic acid, 2% beta-mercaptoethanol in nuclease-free water) (Wang and Stegemann 2010). The samples were then incubated in a water bath at 65 °C for 30 minutes and centrifuged at 1,6000 *g* for 15 minutes. The supernatant was transferred to two new microcentrifuge tubes and added equal volumes of UltraPure™ phenol:chloroform:isoamyl alcohol (25:24:1, Invitrogen). Afterward, the evenly-mixed samples were centrifuged at 1,6000 g for 15 minutes. The supernatant was transferred to a new microcentrifuge tube and mixed with equal volumes of 8M LiCl. Subsequently, the samples were kept in a -20 °C refrigerator for at least 2 hours and then centrifuged at 1,6000 *g* for 30 minutes to remove the supernatant. The pellet was washed with 1 ml 80% ethanol and centrifuged at 1,6000 *g* for 10 minutes. Finally, the pellet was dissolved in 50 µl nuclease-free water.

As for the *VrDet1*, we evaluated the expression using apical meristem at the V0 stage (unifoliate leaves are fully expanded, and the first trifoliate leaves just emerged) following the previous study (Li, et al. 2018). RNA was extracted using the total RNA isolation kit (Novelgene; Cat. No. RT0300). The extracted RNA solution was treated with DNAse I (NEB) and then cleaned up with the LiCl method mentioned above.

cDNA was synthesized from 1 µg of total RNA for each sample using SuperScript IV Reverse Transcriptase (Invitrogen) and then diluted at 1:20. The iQ SYBR Green Supermix (Bio-Rad) was used to perform real-time qPCR. mRNA's relative expression was calculated using the $2^{-\Delta\Delta CT}$ method (Livak and Schmittgen 2001) using the housekeeping gene *VrCYP20* (Li, et al. 2015). The intron-spanning primers were designed for the qPCR experiment (Supplementary Table S5).

Evolutionary and association analyses

We used the coding sequence of *VrMYB26* (LOC106761638) to retrieve its homologous genes in azuki bean (*V. angularis*), cowpea (*V. unguiculata*), common bean (*Phaseolus vulgaris*), and *Arabidopsis thaliana* from public databases, including VigGS (Sakai, et al. 2016), Phytozome (Goodstein, et al. 2012), and TAIR (Huala, et al. 2001). Sequences were aligned, and the maximum-likelihood (ML) tree was constructed with 1,000 bootstrap

621 replications using MEGA v11(Tamura, et al. 2021). In addition, we estimated pairwise
622 d_N/d_S ratios in each clade according to the Yang & Nielsen (2000) method (Yang and
623 Nielsen 2000) with PAML v4.9 (Yang 2007). We constructed neighbor-joining tree of
624 promoter region of targeted genes with ape package in R v4.1.2 (Paradis and Schliep 2018).
625 The haplotype network was constructed using PopART v1.7 with the TCS algorithm
626 (Leigh and Bryant 2015). We used the SNPs without heterozygotes and missing values in
627 the *VrDet1* and *VrMYB26a* promoter regions for the haplotype network analysis and used
628 *V. mungo* as the outgroup.
629

630 ## Acknowledgments

631 We thank Chia-Yu Chen, Pei-Wen Ong, and Jo-Wei Hsieh for the assistance in sample
632 preparation. We are grateful to the support from National Taiwan University's Computer
633 and Information Networking Center for high-performance computing facilities as well as
634 Technology Commons of College of Life Science for molecular biology assistance. C.-R.L.
635 was funded by 107-2923-B-002-004-MY3 and 110-2628-B-002-027 from the Ministry of
636 Science and Technology, Taiwan. C.-T.T. was funded by 107-2923-B-002-004-MY3 from
637 the Ministry of Science and Technology, Taiwan. Y.-P.L. was supported by 110-2313-B-
638 125-001-MY3 from the Ministry of Science and Technology, Taiwan. R.N. and R.S. were
639 funded by the Australian Center for International Agricultural Research (ACIAR) through
640 the projects on International Mungbean Improvement Network (CIM-2014-079 and
641 CROP-2019-144) and by the strategic long-term donors to the World Vegetable Center:
642 Republic of China (Taiwan), UK aid from the UK government, United States Agency for
643 International Development (USAID), Germany, Thailand, Philippines, Korea, and Japan.
644 E.B.-v.-W. was supported by USDA Multistate Hatch NE1710. M.S. was supported by the
645 Ministry of Science and Higher Education of the Russian Federation under the strategic
646 academic leadership program "Priority 2030" (Agreement 075-15-2021-1333 dated
647 30.09.2021). S.N. was supported by the Zumberge foundation.
648

649 ## Author Contributions

C.-R.L. designed and supervised the study. Y.-P.L., H.-W.C., and C.-R.L. performed data analyses and wrote the manuscript with help from other authors. H.-W.C. and P.-M.Y. collected phenotypic data and conducted qPCR experiment. All authors read and approved the manuscript.

Data Availability

The raw sequencing data for each of 114 *Vigna radiata* accessions and 1 *V. mungo* generated in this study have been submitted to the NCBI BioProject database (https://www.ncbi.nlm.nih.gov/bioproject/) under accession number PRJNA838242.

References

Abbo S, van-Oss RP, Gopher A, Saranga Y, Ofner I, Peleg Z. 2014. Plant domestication versus crop evolution: a conceptual framework for cereals and grain legumes. Trends in plant science 19:351-360.

Alexander DH, Novembre J, Lange K. 2009. Fast model-based estimation of ancestry in unrelated individuals. Genome Res 19:1655-1664.

Alonso-Blanco C, Andrade J, Becker C, Bemm F, Bergelson J, Borgwardt KM, Cao J, Chae E, Dezwaan TM, Ding W. 2016. 1,135 genomes reveal the global pattern of polymorphism in Arabidopsis thaliana. Cell 166:481-491.

Bilyeu K, Palavalli L, Sleper D, Beuselinck P. 2005. Mutations in soybean microsomal omega-3 fatty acid desaturase genes reduce linolenic acid concentration in soybean seeds. Crop Science 45:1830-1836.

Bradbury PJ, Zhang Z, Kroon DE, Casstevens TM, Ramdoss Y, Buckler ES. 2007. TASSEL: software for association mapping of complex traits in diverse samples. Bioinformatics 23:2633-2635.

Breria CM, Hsieh CH, Yen J-Y, Nair R, Lin C-Y, Huang S-M, Noble TJ, Schafleitner R. 2020. Population structure of the world vegetable center mungbean mini core collection and genome-wide association mapping of loci associated with variation of seed coat luster. Tropical Plant Biology 13:1-12.

Camacho C, Coulouris G, Avagyan V, Ma N, Papadopoulos J, Bealer K, Madden TL. 2009. BLAST+: architecture and applications. BMC bioinformatics 10:1-9.

Castillo C, Fuller DQ. 2010. Still too fragmentary and dependent upon chance? Advances in the study of early Southeast Asian archaeobotany. Fifty years of archaeology in Southeast Asia: Essays in honour of Ian Glover:91-111.

Chauhan YS, Williams R. 2018. Physiological and agronomic strategies to increase mungbean yield in climatically variable environments of Northern Australia. Agronomy 8:83.

Chen C, Chen H, Zhang Y, Thomas HR, Frank MH, He Y, Xia R. 2020. TBtools: an integrative toolkit developed for interactive analyses of big biological data. Molecular plant 13:1194-1202.

Chen H, Wang L, Wang S, Liu C, Blair MW, Cheng X. 2015. Transcriptome sequencing of mung bean (Vigna radiate L.) genes and the identification of EST-SSR markers. PloS one 10:e0120273.

Chen L-T. 1980. A study of the systems of rotating crops in Chinese history. Bulletin of the Institute of History and Philology 51:281-313.

Cingolani P, Platts A, Wang le L, Coon M, Nguyen T, Wang L, Land SJ, Lu X, Ruden DM. 2012. A program for annotating and predicting the effects of single nucleotide polymorphisms, SnpEff: SNPs in the genome of Drosophila melanogaster strain w1118; iso-2; iso-3. Fly (Austin) 6:80-92.

Cox MP, Peterson DA, Biggs PJ. 2010. SolexaQA: At-a-glance quality assessment of Illumina second-generation sequencing data. BMC bioinformatics 11:485.

Danecek P, Auton A, Abecasis G, Albers CA, Banks E, DePristo MA, Handsaker RE, Lunter G, Marth GT, Sherry ST, et al. 2011. The variant call format and VCFtools. Bioinformatics 27:2156-2158.

Depenbusch L, Farnworth CR, Schreinemachers P, Myint T, Islam MM, Kundu ND, Myint T, San AM, Jahan R, Nair RM. 2021. When Machines Take the Beans: Ex-Ante Socioeconomic Impact Evaluation of Mechanized Harvesting of Mungbean in Bangladesh and Myanmar. Agronomy 11:925.

Di Vittori V, Bitocchi E, Rodriguez M, Alseekh S, Bellucci E, Nanni L, Gioia T, Marzario S, Logozzo G, Rossato M. 2021. Pod indehiscence in common bean is associated with the fine regulation of PvMYB26. Journal of experimental botany 72:1617-1633.

Doebley J, Stec A, Gustus C. 1995. teosinte branched1 and the origin of maize: evidence for epistasis and the evolution of dominance. Genetics 141:333-346.

Eshed Y, Lippman ZB. 2019. Revolutions in agriculture chart a course for targeted breeding of old and new crops. science 366:eaax0025.

Fuller DQ. 2007. Contrasting patterns in crop domestication and domestication rates: recent archaeobotanical insights from the Old World. Annals of Botany 100:903-924.

Fuller DQ, Allaby R. 2018. Seed dispersal and crop domestication: shattering, germination and seasonality in evolution under cultivation. Annual Plant Reviews online:238-295.

Fuller DQ, Harvey EL. 2006. The archaeobotany of Indian pulses: identification, processing and evidence for cultivation. Environmental archaeology 11:219-246.

Garud NR, Messer PW, Buzbas EO, Petrov DA. 2015. Recent selective sweeps in North American Drosophila melanogaster show signatures of soft sweeps. PLoS genetics 11:e1005004.

Giovannoni J. 2018. Tomato multiomics reveals consequences of crop domestication and improvement. Cell 172:6-8.

Goodstein DM, Shu S, Howson R, Neupane R, Hayes RD, Fazo J, Mitros T, Dirks W, Hellsten U, Putnam N. 2012. Phytozome: a comparative platform for green plant genomics. Nucleic acids research 40:D1178-D1186.

Haas BJ, Papanicolaou A, Yassour M, Grabherr M, Blood PD, Bowden J, Couger MB, Eccles D, Li B, Lieber M. 2013. De novo transcript sequence reconstruction from RNA-seq using the Trinity platform for reference generation and analysis. Nature protocols 8:1494-1512.

Haas BJ, Salzberg SL, Zhu W, Pertea M, Allen JE, Orvis J, White O, Buell CR, Wortman JR. 2008. Automated eukaryotic gene structure annotation using EVidenceModeler and the Program to Assemble Spliced Alignments. Genome biology 9:1-22.

Harris AM, Garud NR, DeGiorgio M. 2018. Detection and classification of hard and soft sweeps from unphased genotypes by multilocus genotype identity. Genetics 210:1429-1452.

740 Hewavitharane H, Warnakulasooriya H, Wajira Kumara G. 2010. Constraints to expansion
741 of cowpea and mungbean under rain-fed farming in Anuradhapura District. In.
742 Hirano H. 2021. Basic 7S globulin in plants. Journal of Proteomics 240:104209.
743 Huala E, Dickerman AW, Garcia-Hernandez M, Weems D, Reiser L, LaFond F, Hanley D,
744 Kiphart D, Zhuang M, Huang W. 2001. The Arabidopsis Information Resource (TAIR): a
745 comprehensive database and web-based information retrieval, analysis, and visualization
746 system for a model plant. Nucleic acids research 29:102-105.
747 Huang X, Kurata N, Wang Z-X, Wang A, Zhao Q, Zhao Y, Liu K, Lu H, Li W, Guo Y.
748 2012. A map of rice genome variation reveals the origin of cultivated rice. Nature 490:497-
749 501.
750 Huang X, Zhao Y, Li C, Wang A, Zhao Q, Li W, Guo Y, Deng L, Zhu C, Fan D. 2012.
751 Genome-wide association study of flowering time and grain yield traits in a worldwide
752 collection of rice germplasm. Nature genetics 44:32-39.
753 Huerta-Cepas J, Forslund K, Coelho LP, Szklarczyk D, Jensen LJ, Von Mering C, Bork P.
754 2017. Fast genome-wide functional annotation through orthology assignment by eggNOG-
755 mapper. Molecular biology and evolution 34:2115-2122.
756 Hufford MB, Xu X, Van Heerwaarden J, Pyhäjärvi T, Chia J-M, Cartwright RA, Elshire
757 RJ, Glaubitz JC, Guill KE, Kaeppler SM. 2012. Comparative population genomics of
758 maize domestication and improvement. Nature genetics 44:808-811.
759 Huson DH, Bryant D. 2006. Application of phylogenetic networks in evolutionary studies.
760 Molecular biology and evolution 23:254-267.
761 Huyghe C. 1998. Genetics and genetic modifications of plant architecture in grain legumes:
762 a review. Agronomie 18:383-411.
763 Isemura T, Kaga A, Tabata S, Somta P, Srinives P, Shimizu T, Jo U, Vaughan DA,
764 Tomooka N. 2012. Construction of a genetic linkage map and genetic analysis of
765 domestication related traits in mungbean (Vigna radiata).
766 Janczarek M, Rachwał K, Marzec A, Grządziel J, Palusińska-Szysz M. 2015. Signal
767 molecules and cell-surface components involved in early stages of the legume–rhizobium
768 interactions. Applied Soil Ecology 85:94-113.
769 Kaga A, Shimizu T, Watanabe S, Tsubokura Y, Katayose Y, Harada K, Vaughan DA,
770 Tomooka N. 2012. Evaluation of soybean germplasm conserved in NIAS genebank and
771 development of mini core collections. Breeding science 61:566-592.
772 Kang YJ, Kim SK, Kim MY, Lestari P, Kim KH, Ha BK, Jun TH, Hwang WJ, Lee T, Lee
773 J, et al. 2014. Genome sequence of mungbean and insights into evolution within Vigna
774 species. Nat Commun 5:5443.
775 Kato S, Fujii K, Yumoto S, Ishimoto M, Shiraiwa T, Sayama T, Kikuchi A, Nishio T. 2015.
776 Seed yield and its components of indeterminate and determinate lines in recombinant
777 inbred lines of soybean. Breeding science 65:154-160.

778 Kato S, Sayama T, Taguchi-Shiobara F, Kikuchi A, Ishimoto M, Cober E. 2019. Effect of
779 change from a determinate to a semi-determinate growth habit on the yield and lodging
780 resistance of soybeans in the northeast region of Japan. Breeding science 69:151-159.
781 Kilgore-Norquest L, Sneller C. 2000. Effect of stem termination on soybean traits in
782 southern US production systems. Crop Science 40:83-90.
783 Kim D, Langmead B, Salzberg SL. 2015. HISAT: a fast spliced aligner with low memory
784 requirements. Nature methods 12:357-360.
785 Kim M-S, Lozano R, Kim JH, Bae DN, Kim S-T, Park J-H, Choi MS, Kim J, Ok H-C,
786 Park S-K. 2021. The patterns of deleterious mutations during the domestication of soybean.
787 Nature communications 12:1-14.
788 Kumar R, Sharma V, Suresh S, Ramrao DP, Veershetty A, Kumar S, Priscilla K, Hangargi
789 B, Narasanna R, Pandey MK. 2021. Understanding Omics Driven Plant Improvement and
790 de novo Crop Domestication: Some Examples. Frontiers in genetics:415.
791 Lawn R. 1989. Agronomic and physiological constraints to the productivity of tropical
792 grain legumes and prospects for improvement. Experimental Agriculture 25:509-528.
793 Lawn R, Rebetzke G. 2006. Variation among Australian accessions of the wild mungbean
794 (Vigna radiata ssp. sublobata) for traits of agronomic, adaptive, or taxonomic interest.
795 Australian Journal of Agricultural Research 57:119-132.
796 Lawn RJ, Cottrell A, Pastures CLSLQ editors.; 1988.
797 Leigh JW, Bryant D. 2015. popart: full-feature software for haplotype network construction.
798 Methods in Ecology and Evolution 6:1110-1116.
799 Li C, Zhou A, Sang T. 2006. Rice domestication by reducing shattering. science 311:1936-
800 1939.
801 Li H, Durbin R. 2009. Fast and accurate short read alignment with Burrows-Wheeler
802 transform. Bioinformatics 25:1754-1760.
803 Li S. 2016. The Ben Cao Gang Mu. In. The Ben Cao Gang Mu: University of California
804 Press.
805 Li S, Ding Y, Zhang D, Wang X, Tang X, Dai D, Jin H, Lee SH, Cai C, Ma J. 2018. Parallel
806 domestication with a broad mutational spectrum of determinate stem growth habit in
807 leguminous crops. The Plant Journal 96:761-771.
808 Li S-W, Shi R-F, Leng Y. 2015. De novo characterization of the mung bean transcriptome
809 and transcriptomic analysis of adventitious rooting in seedlings using RNA-Seq. PloS one
810 10:e0132969.
811 Li Y-h, Zhao S-c, Ma J-x, Li D, Yan L, Li J, Qi X-t, Guo X-s, Zhang L, He W-m. 2013.
812 Molecular footprints of domestication and improvement in soybean revealed by whole
813 genome re-sequencing. BMC genomics 14:1-12.
814 Liu G, Zhao L, Averitt BJ, Liu Y, Zhang B, Chang R, Ma Y, Luan X, Guan R, Qiu L. 2015.
815 Geographical distribution of GmTfl1 alleles in Chinese soybean varieties. The Crop
816 Journal 3:371-378.

817 Liu H, Li Q, Xing Y. 2018. Genes contributing to domestication of rice seed traits and its
818 global expansion. Genes 9:489.
819 Liu MS, Kuo TC, Ko CY, Wu DC, Li KY, Lin WJ, Lin CP, Wang YW, Schafleitner R, Lo
820 HF, et al. 2016. Genomic and transcriptomic comparison of nucleotide variations for
821 insights into bruchid resistance of mungbean (Vigna radiata [L.] R. Wilczek). BMC Plant
822 Biol 16:46.
823 Livak KJ, Schmittgen TD. 2001. Analysis of relative gene expression data using real-time
824 quantitative PCR and the 2− ΔΔCT method. methods 25:402-408.
825 Mangini G, Blanco A, Nigro D, Signorile MA, Simeone R. 2021. Candidate genes and
826 quantitative trait loci for grain yield and seed size in durum wheat. Plants 10:312.
827 Marcott SA, Shakun JD, Clark PU, Mix AC. 2013. A reconstruction of regional and global
828 temperature for the past 11,300 years. science 339:1198-1201.
829 Martin M. 2011. Cutadapt removes adapter sequences from high-throughput sequencing
830 reads. EMBnet. journal 17:10-12.
831 McKenna A, Hanna M, Banks E, Sivachenko A, Cibulskis K, Kernytsky A, Garimella K,
832 Altshuler D, Gabriel S, Daly M. 2010. The Genome Analysis Toolkit: a MapReduce
833 framework for analyzing next-generation DNA sequencing data. Genome research
834 20:1297-1303.
835 Mendoza EMT, Adachi M, Bernardo AEN, Utsumi S. 2001. Mungbean [Vigna radiata (L.)
836 Wilczek] globulins: purification and characterization. Journal of Agricultural and Food
837 Chemistry 49:1552-1558.
838 Meyer RS, Purugganan MD. 2013. Evolution of crop species: genetics of domestication
839 and diversification. Nature reviews genetics 14:840-852.
840 Nair RM, Schafleitner R, Lee S-H. 2020. The mungbean genome: Springer.
841 Nguyen TD, Lawn R, Bielig L. 2012. Expression and inheritance of perenniality and other
842 qualitative traits in hybrids between mungbean cultivars and Australian wild accessions.
843 Crop and Pasture Science 63:619-634.
844 Noble TJ, Tao Y, Mace ES, Williams B, Jordan DR, Douglas CA, Mundree SG. 2018.
845 Characterization of linkage disequilibrium and population structure in a mungbean
846 diversity panel. Frontiers in plant science 8:2102.
847 Norihiko T, Kaga A, Isemura T, Vaughan D, Srinives P, Somta P, Thadavong S,
848 Bounphanousay C, Kanyavong K, Inthapanya P editors. Proceeding of the14th NIAS
849 international workshop on Genetic Resources, Genetic and Comparative Genomics of
850 Legumes (Glycine and Vigna). 2010.
851 Paradis E, Schliep K. 2018. ape 5.0: an environment for modern phylogenetics and
852 evolutionary analyses in R. Bioinformatics 35:526-528.
853 Parker TA, Lo S, Gepts P. 2021. Pod shattering in grain legumes: emerging genetic and
854 environment-related patterns. The Plant Cell 33:179-199.

855 Pavlidis P, Živković D, Stamatakis A, Alachiotis N. 2013. SweeD: likelihood-based
856 detection of selective sweeps in thousands of genomes. Molecular biology and evolution
857 30:2224-2234.
858 Pertea M, Pertea GM, Antonescu CM, Chang T-C, Mendell JT, Salzberg SL. 2015.
859 StringTie enables improved reconstruction of a transcriptome from RNA-seq reads. Nature
860 biotechnology 33:290-295.
861 Pham A-T, Shannon JG, Bilyeu KD. 2012. Combinations of mutant FAD2 and FAD3
862 genes to produce high oleic acid and low linolenic acid soybean oil. Theoretical and
863 Applied Genetics 125:503-515.
864 Phillips SJ, Anderson RP, Schapire RE. 2006. Maximum entropy modeling of species
865 geographic distributions. Ecological Modelling 190:231-259.
866 Pierce BA. 2012. Genetics: A Conceptual Approach: W. H. Freeman.
867 Pomar F, Merino F, Barceló AR. 2002. O-4-Linked coniferyl and sinapyl aldehydes in
868 lignifying cell walls are the main targets of the Wiesner (phloroglucinol-HCl) reaction.
869 Protoplasma 220:0017-0028.
870 Purcell S, Neale B, Todd-Brown K, Thomas L, Ferreira MA, Bender D, Maller J, Sklar P,
871 De Bakker PI, Daly MJ. 2007. PLINK: a tool set for whole-genome association and
872 population-based linkage analyses. The American journal of human genetics 81:559-575.
873 Purugganan MD, Fuller DQ. 2009. The nature of selection during plant domestication.
874 Nature 457:843-848.
875 Roucou A, Violle C, Fort F, Roumet P, Ecarnot M, Vile D. 2018. Shifts in plant functional
876 strategies over the course of wheat domestication. Journal of Applied Ecology 55:25-37.
877 Sakai H, Naito K, Takahashi Y, Sato T, Yamamoto T, Muto I, Itoh T, Tomooka N. 2016.
878 The Vigna Genome Server,'Vig GS': A genomic knowledge base of the genus Vigna based
879 on high-quality, annotated genome sequence of the Azuki Bean, Vigna angularis (Willd.)
880 Ohwi & Ohashi. Plant and Cell Physiology 57:e2-e2.
881 Schouten HJ, Tikunov Y, Verkerke W, Finkers R, Bovy A, Bai Y, Visser RG. 2019.
882 Breeding has increased the diversity of cultivated tomato in The Netherlands. Frontiers in
883 plant science:1606.
884 Slater GSC, Birney E. 2005. Automated generation of heuristics for biological sequence
885 comparison. BMC bioinformatics 6:1-11.
886 Song Y, Sun E-tZ, Sun S-C. 1997. Chinese technology in the seventeenth century: Courier
887 Corporation.
888 Specht JE, Diers BW, Nelson RL, de Toledo JFF, Torrion JA, Grassini P. 2014. Soybean.
889 Yield gains in major US field crops 33:311-355.
890 Stanke M, Keller O, Gunduz I, Hayes A, Waack S, Morgenstern B. 2006. AUGUSTUS:
891 ab initio prediction of alternative transcripts. Nucleic acids research 34:W435-W439.
892 Takahashi Y, Kongjaimun A, Muto C, Kobayashi Y, Kumagai M, Sakai H, Satou K,
893 Teruya K, Shiroma A, Shimoji M. 2020. Same locus for non-shattering seed pod in two

894 independently domesticated legumes, Vigna angularis and Vigna unguiculata. Frontiers in
895 genetics 11:748.
896 Tamura K, Stecher G, Kumar S. 2021. MEGA11: molecular evolutionary genetics analysis
897 version 11. Molecular biology and evolution 38:3022-3027.
898 Tateishi Y. 1996. Systematics of the species of Vigna subgenus Ceratotropis. Mungbean
899 Germplasm: collection and utilization for breeding program.:9-24.
900 Terhorst J, Kamm JA, Song YS. 2017. Robust and scalable inference of population history
901 from hundreds of unphased whole genomes. Nat Genet 49:303-309.
902 Tobler R, Rohrlach A, Soubrier J, Bover P, Llamas B, Tuke J, Bean N, Abdullah-Highfold
903 A, Agius S, O'Donoghue A. 2017. Aboriginal mitogenomes reveal 50,000 years of
904 regionalism in Australia. Nature 544:180-184.
905 Van Bel M, Diels T, Vancaester E, Kreft L, Botzki A, Van de Peer Y, Coppens F,
906 Vandepoele K. 2018. PLAZA 4.0: an integrative resource for functional, evolutionary and
907 comparative plant genomics. Nucleic acids research 46:D1190-D1196.
908 Van der Auwera GA, Carneiro MO, Hartl C, Poplin R, Del Angel G, Levy-Moonshine A,
909 Jordan T, Shakir K, Roazen D, Thibault J. 2013. From FastQ data to high-confidence
910 variant calls: the genome analysis toolkit best practices pipeline. Current protocols in
911 bioinformatics 43:11.10. 11-11.10. 33.
912 Vavilov NI. 1922. The law of homologous series in variation. Journal of genetics 12:47-
913 89.
914 Vavilov NI. 1951. The origin, variation, immunity and breeding of cultivated plants: LWW.
915 von Wettberg EJB, Chang PL, Basdemir F, Carrasquila-Garcia N, Korbu LB, Moenga SM,
916 Bedada G, Greenlon A, Moriuchi KS, Singh V, et al. 2018. Ecology and genomics of an
917 important crop wild relative as a prelude to agricultural innovation. Nat Commun 9:649.
918 Wang L, Stegemann JP. 2010. Extraction of high quality RNA from polysaccharide
919 matrices using cetlytrimethylammonium bromide. Biomaterials 31:1612-1618.
920 Xia Z, Watanabe S, Yamada T, Tsubokura Y, Nakashima H, Zhai H, Anai T, Sato S,
921 Yamazaki T, Lü S. 2012. Positional cloning and characterization reveal the molecular basis
922 for soybean maturity locus E1 that regulates photoperiodic flowering. Proceedings of the
923 National Academy of Sciences 109:E2155-E2164.
924 Xie M, Zhang J, Tschaplinski TJ, Tuskan GA, Chen J-G, Muchero W. 2018. Regulation of
925 lignin biosynthesis and its role in growth-defense tradeoffs. Frontiers in plant science:1427.
926 Yang Z. 2007. PAML 4: phylogenetic analysis by maximum likelihood. Molecular biology
927 and evolution 24:1586-1591.
928 Yang Z, Nielsen R. 2000. Estimating synonymous and nonsynonymous substitution rates
929 under realistic evolutionary models. Molecular biology and evolution 17:32-43.
930 Zhang C, Dong S-S, Xu J-Y, He W-M, Yang T-L. 2019. PopLDdecay: a fast and effective
931 tool for linkage disequilibrium decay analysis based on variant call format files.
932 Bioinformatics 35:1786-1788.

933 Zhang J, Song Q, Cregan PB, Nelson RL, Wang X, Wu J, Jiang G-L. 2015. Genome-wide
934 association study for flowering time, maturity dates and plant height in early maturing
935 soybean (Glycine max) germplasm. BMC genomics 16:1-11.
936 Zhou Z, Jiang Y, Wang Z, Gou Z, Lyu J, Li W, Yu Y, Shu L, Zhao Y, Ma Y. 2015.
937 Resequencing 302 wild and cultivated accessions identifies genes related to domestication
938 and improvement in soybean. Nature biotechnology 33:408-414.

939
940

Supplementary figures

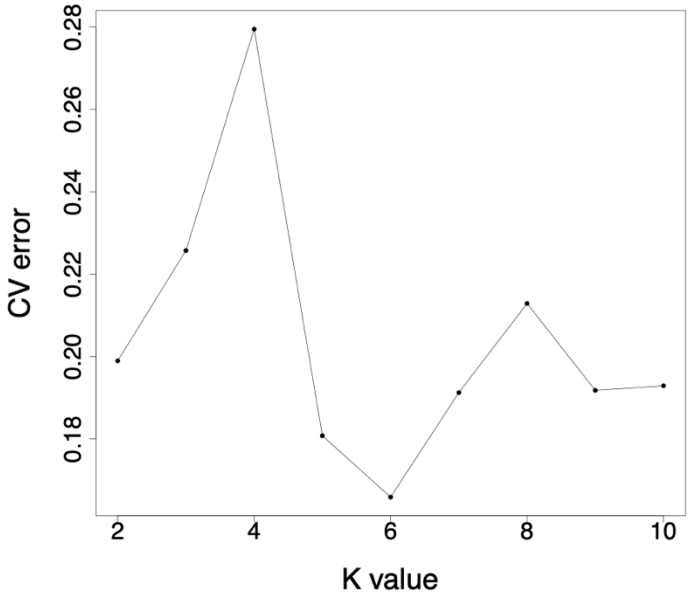

Supplementary Fig. S1. Cross-validation error of each K value.

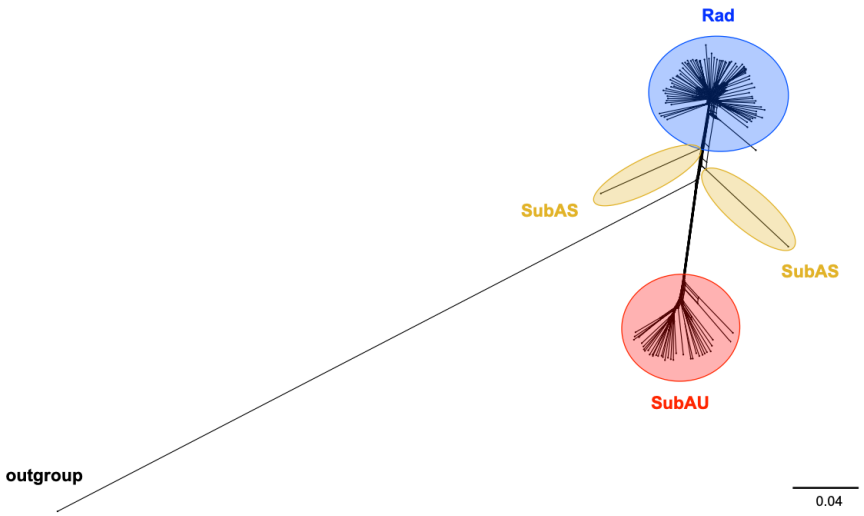

Supplementary Fig. S2. Phylogenetic network of the 114 mungbean accessions and one outgroup.

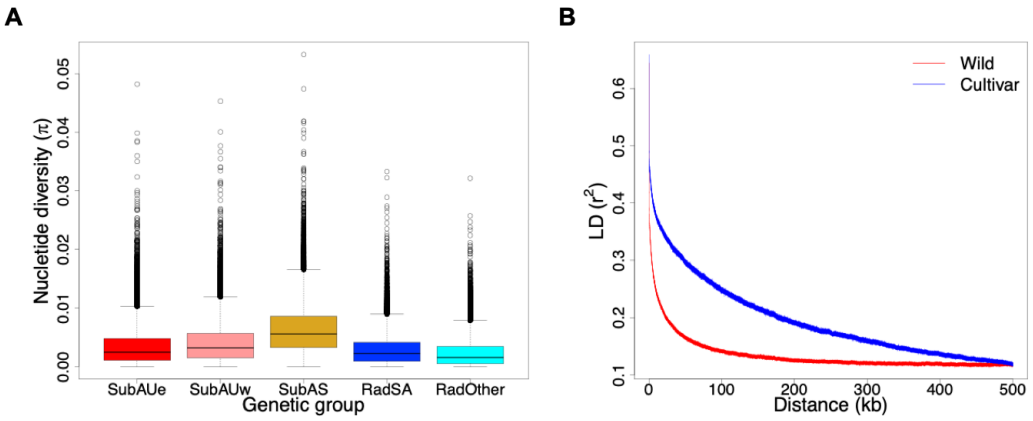

Supplementary Fig. S3. Genetic diversity of mungbean. (A) Nucleotide diversity (π) in the 10kb window of the three wild genetic groups (SubAUe, SubAUw, and SubAS) and the two cultivated genetic groups (RadSA and RadOther). The boxes indicate medians and interquartile ranges, whiskers indicate 95% values, and additional points in each boxplot represent outliers. (B) Decay of linkage disequilibrium (LD) of wild and cultivated populations.

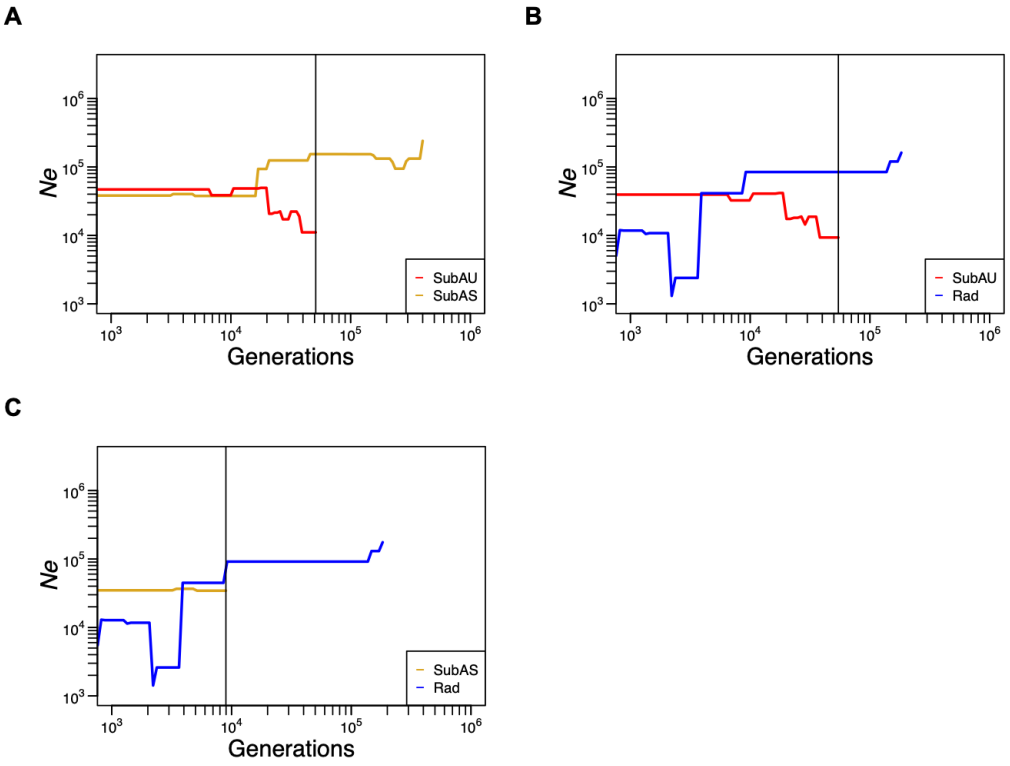

Supplementary Fig. S4. Pairwise population divergence time. (A) SubAU and SubAS (B) SubAU and Rad (C) SubAS and Rad. The vertical black lines denote the estimated divergence time.

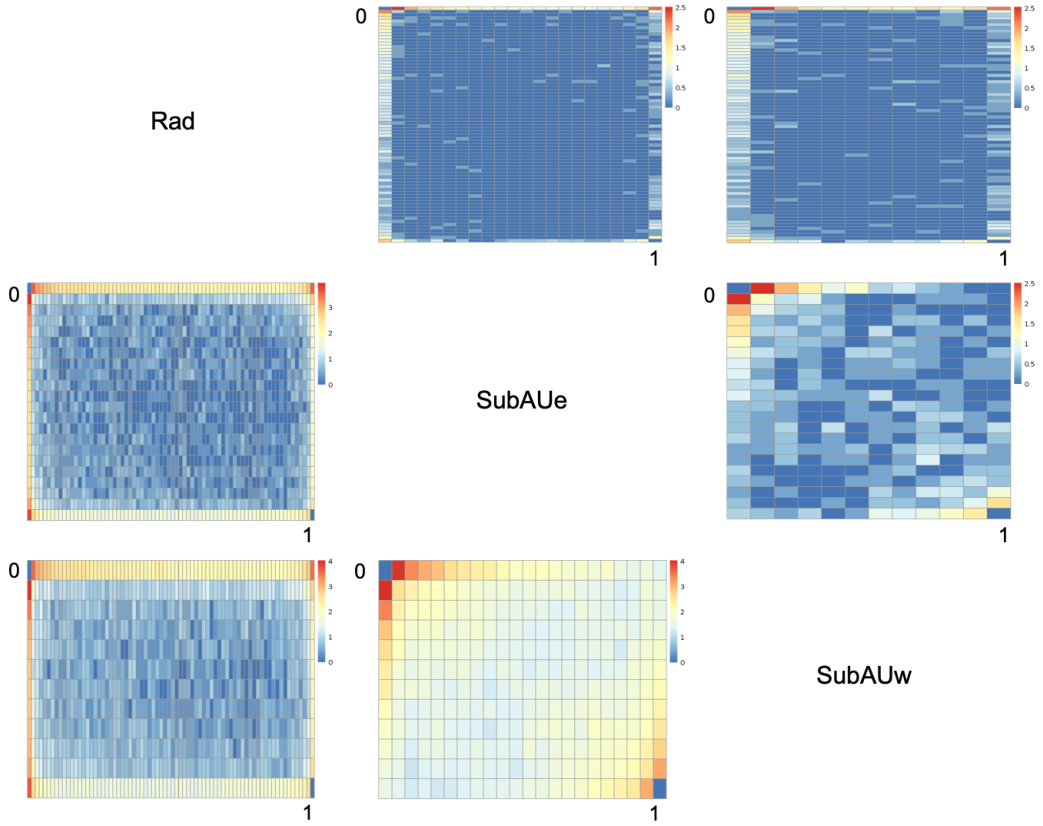

Supplementary Fig. S5. Two-dimensional site frequency spectrum (2D SFS) between Rad, SubAUe, and SubAUw groups. The upper triangle plots are 2D SFS of the SNPs with high impact estimated by SnpEff; the lower triangle plots are the 2D SFS of the 4-fold degenerate SNPs. Colors reflect the log10 number of SNPs.

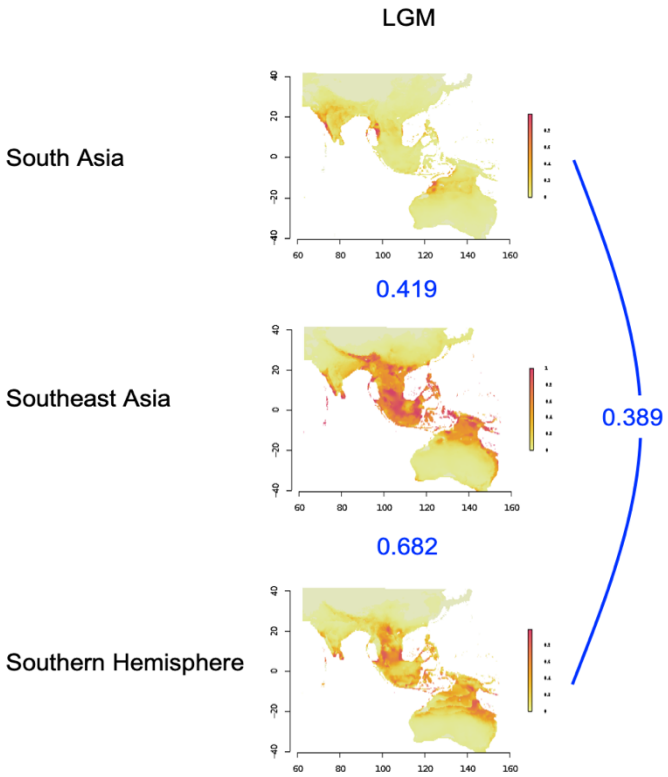

966
967 **Supplementary Fig. S6. Ecological niche modeling of suitable habitats for the wild**
968 **mungbean populations in South Asia, Southeast Asia, and South Hemisphere in Last**
969 **Glacial Maximum (22 kya).** Colors represent niche suitability. The three graphs (South
970 Asia, Southeast Asia, and Southern Hemisphere) represent niche models constructed from
971 the presence data of wild mungbean from these regions and projected to the whole
972 geographical extent. Data of the Last Glacial Maximum (22 kya, LGM) was based on the
973 circulation model of CCSM4. The numbers in blue between pairs of modeled distribution
974 indicate the Schoner'D values, where higher values represent higher niche similarity.

975

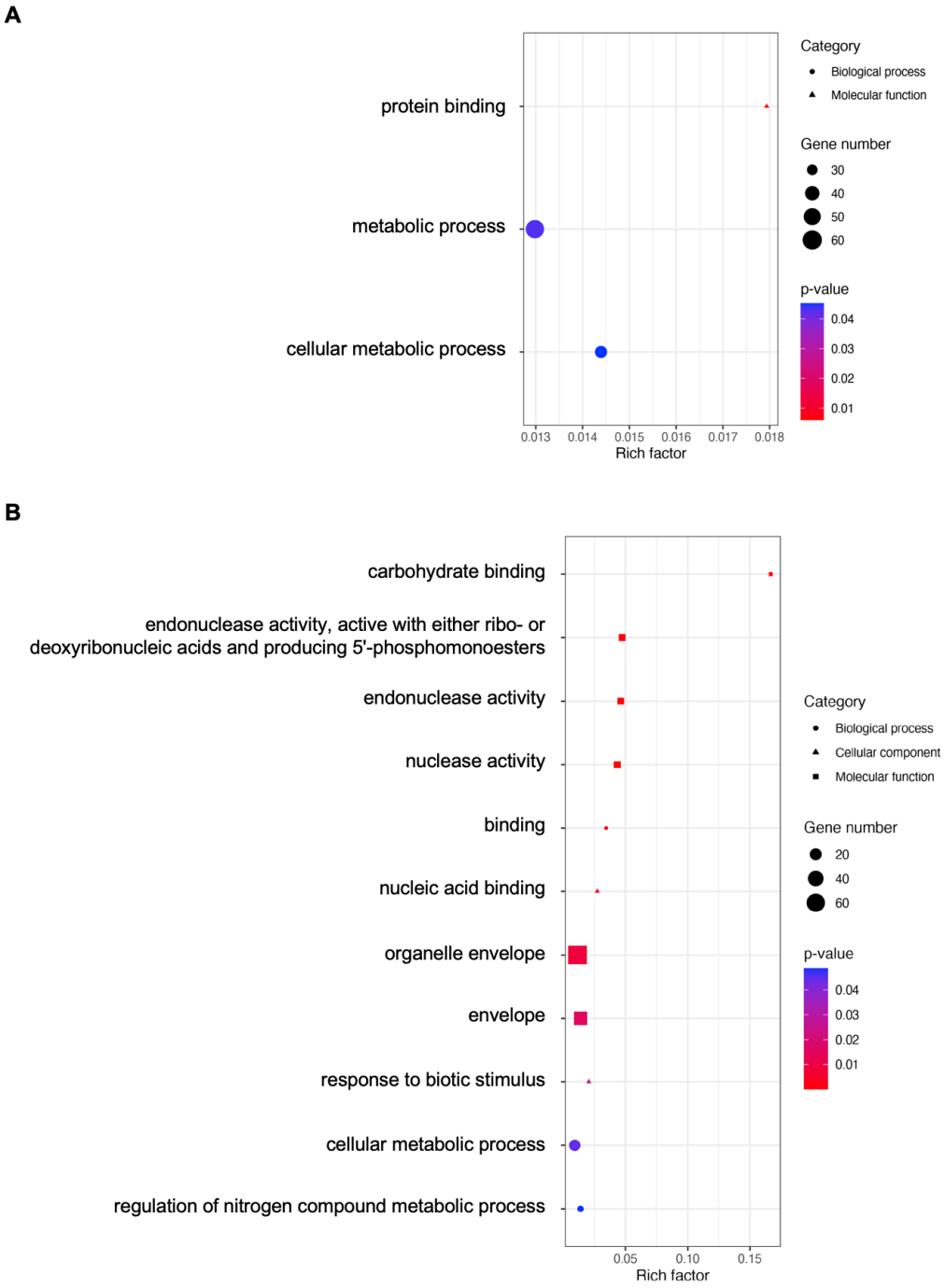

Supplementary Fig. S7. Gene Ontology (GO) enrichment of candidate genes in the regions of signatures of selection. Shown are the GO enrichment of candidate selective sweep genes from the (A) composite likelihood ratio (CLR) of the wild group, (B) CLR of the cultivars, and (C) reduction of diversity.

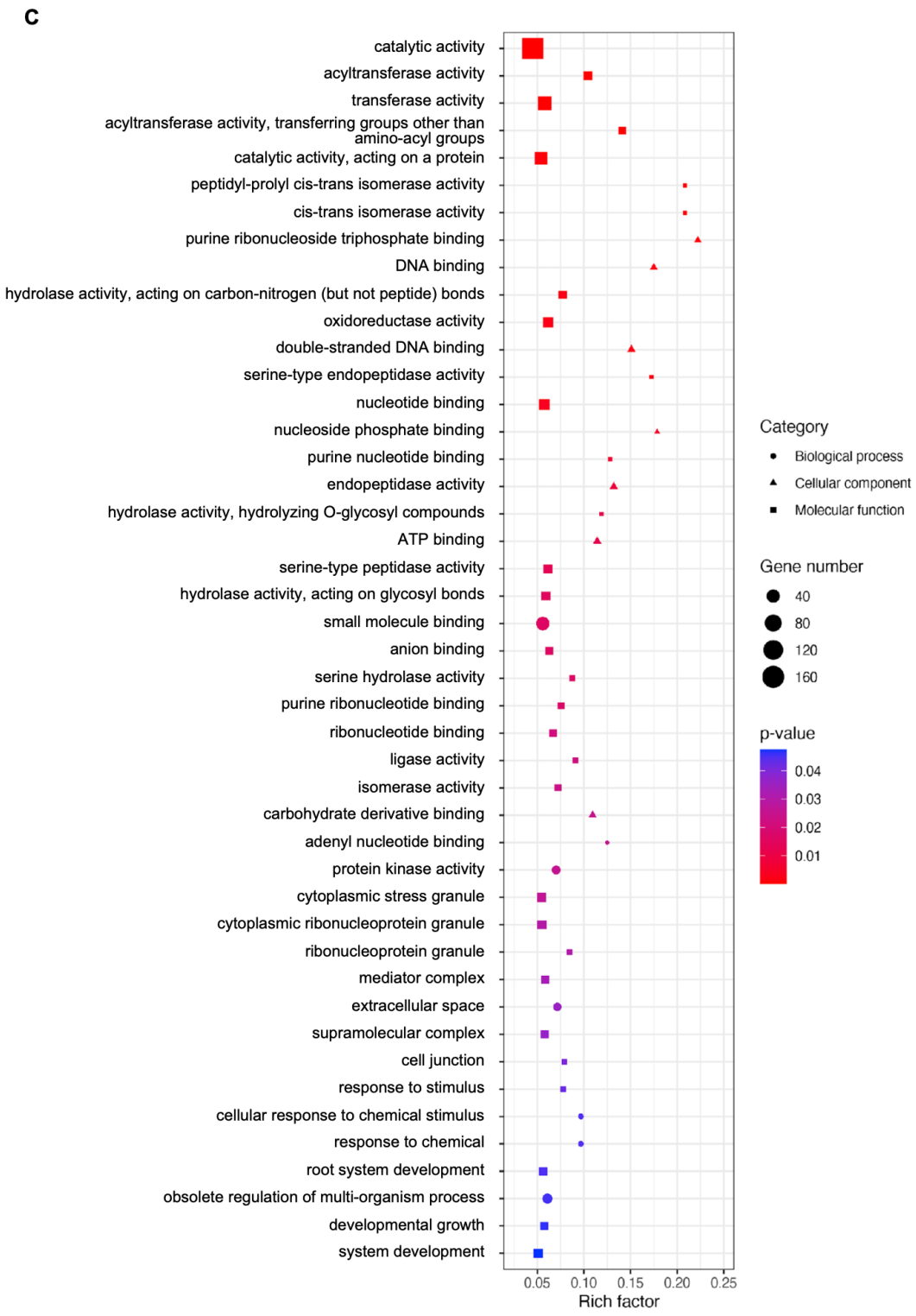

982

983 **Supplementary Fig. S7 (Continue).**

984

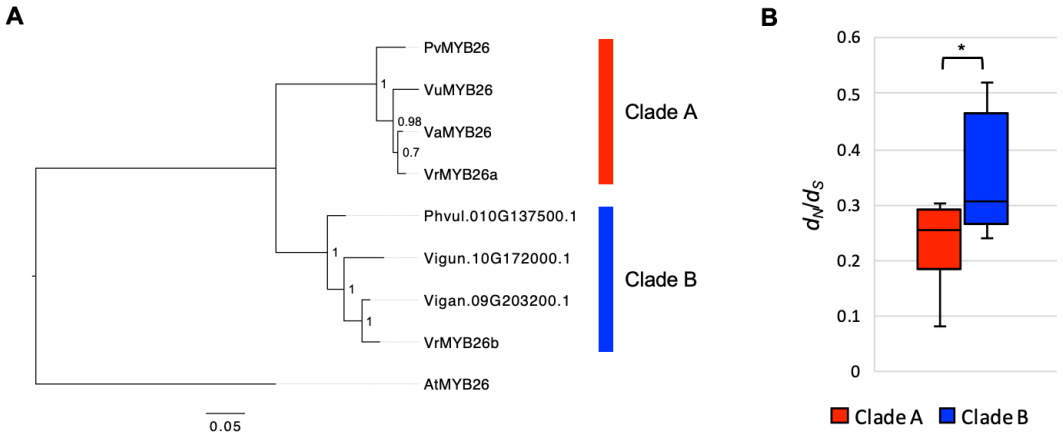

985

986 **Supplementary Fig. S8. Evolution of *MYB26* homologs in legumes.** (A) Maximum-
987 likelihood (ML) tree constructed from the coding sequences of the *MYB26* homologs using
988 *AtMYB26* as an outgroup. The numbers adjacent to nodes indicate the proportion of support
989 in 1,000 bootstrap re-samplings. (B) The d_N/d_S ratios of the *MYB26* orthologs are estimated
990 based on the pairwise comparison in each of the two clades in the ML tree. The boxes
991 indicate medians and interquartile ranges; the whiskers indicate 95% values (* indicates p
992 value < 0.05).

993

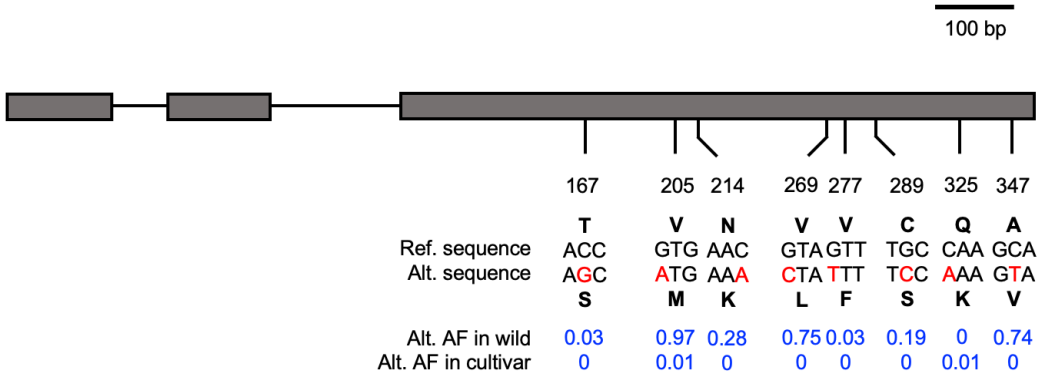

994

995 **Supplementary Fig. S9. Diagram of the *VrMYB26a* non-synonymous changes.** Shown
996 are the positions of non-synonymous SNPs and the frequency of alternative alleles (Alt.
997 AF) in wild and cultivated populations.

998

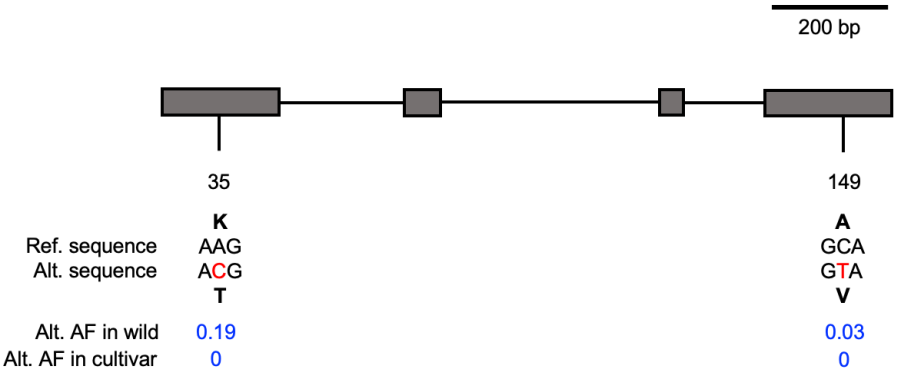

Supplementary Fig. S10. Diagram of the *VrDet1* non-synonymous changes. Shown are the positions of non-synonymous SNPs and the frequency of alternative alleles (Alt. AF) in wild and cultivated populations.

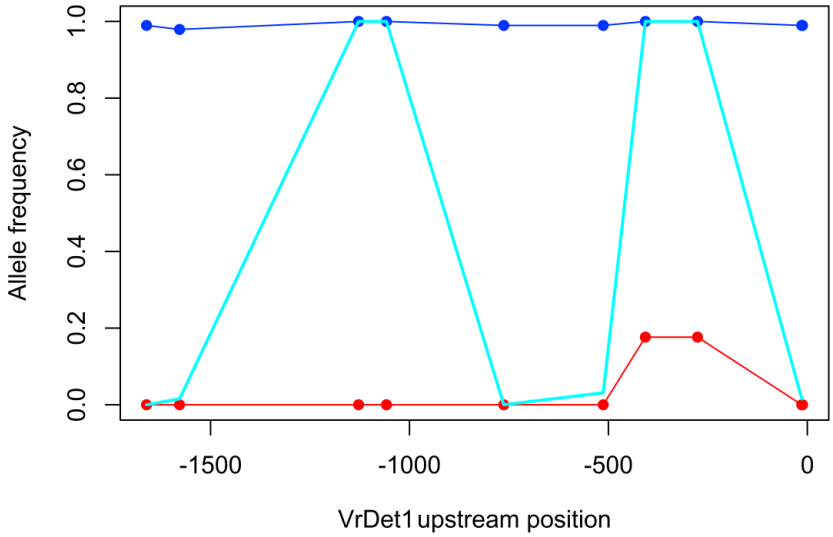

Supplementary Fig. S11. Distribution of allele frequency in *VrDet1* upstream 2kb region among three clades (red: Clade I, sky-blue: Clade II, blue: Clade III). Nine diagnostic SNPs with the large allele frequency differences between Clade I and III were shown, and the major allele in Clade III was used to estimate allele frequency.

Supplementary tables

Supplementary Table S1. Summary of sequencing data for each accession analyzed in this study

Accession	Average base quality	Total reads	Total bases	Mapping reads	Read mapping rate (%)	Sequencing depth (X)
Crystal	38.6	196483180	28727374463	195351734	99.42	62.03
NAM1	39	127533934	19010063503	119996800	94.09	41.05
NAM2	39	126703124	18890287992	122616672	96.77	40.79
NAM3	38.7	148349752	22112564826	144734909	97.56	47.75
NAM4	38.5	94156396	14016993080	93171459	98.95	30.27
NAM5	38.8	119703610	17821660108	116774122	97.55	38.48
NAM6	39	124431120	18546889117	122036022	98.08	40.05
NAM7	39.1	146988240	21900082222	146066498	99.37	47.29
NAM8	39	114165632	17000285477	111296904	97.49	36.71
NAM9	38.3	114995514	17175168161	111740019	97.17	37.09
NAM10	38.7	147767224	22062903874	144915289	98.07	47.64
NAM11	38.5	129858206	19387275676	124465045	95.85	41.87
NAM12	38.4	162972618	24344134422	156681072	96.14	52.57

NAM13	38.6	142539446	21285763164	136730232	95.92	45.97
NAM15	38.5	134863986	20121555751	131533360	97.53	43.45
NAM16	38.7	85364434	12748587321	84299239	98.75	27.53
NAM17	38.1	134722504	20147479994	133167359	98.85	43.51
NAM18	38.7	141671450	21158317508	140643256	99.27	45.69
NAM19	38.4	112779164	16813978606	111409295	98.79	36.31
NAM20	38.5	130499886	19490475112	129397877	99.16	42.09
NAM21	38.6	132985114	19856334359	131512282	98.89	42.88
NAM22	38.4	107398574	16050627709	105897481	98.60	34.66
NAM23	38.9	143669612	21454673884	142409613	99.12	46.33
NAM24	38.3	131334734	19410296478	129409725	98.53	41.92
NAM26	38.1	114831936	16962317946	113213499	98.59	36.63
NAM27	38.1	126707904	18693602904	125423094	98.99	40.37
VI000020AY	38.3	107685230	15714113847	107149544	99.50	33.93
VI000099AG	37.9	123351108	18172014038	121695136	98.66	39.24
VI000232AG	37.9	115094024	16952613959	114295135	99.31	36.61
VI000238AG	38	117628680	17337135019	116884614	99.37	37.44

VI000542BY	37.9	114540288	16892176117	113376374	98.98	36.48
VI000578AG	37.9	140304700	20699908970	139324816	99.30	44.70
VI000625B-BR	38	110947438	16362038748	110341377	99.45	35.33
VI000938AG	38.1	113916038	16771866336	113054013	99.24	36.22
VI001191BG	39	91140902	13357067934	90567830	99.37	28.84
VI001435AG	38	117448760	17467476874	115727581	98.53	37.72
VI001509AG	38.2	108920614	16166073569	108153675	99.30	34.91
VI001514AG	38.6	97989586	14525965237	95722966	97.69	31.37
VI001728AG	38.7	99679194	14672353144	99014305	99.33	31.68
VI001806BG	38.5	107456990	15849661425	106402936	99.02	34.23
VI002176BG	38.6	103202330	15192308217	102428510	99.25	32.81
VI002197BG	38.3	106389320	15792270028	105625140	99.28	34.10
VI002239AG	38.7	100855684	14857800232	100096208	99.25	32.08
VI002456AG	38.8	105440890	15528929567	104898680	99.49	33.53
VI002647AG	38.7	116052796	17101843320	114535313	98.69	36.93
VI002859BG	38.6	99282868	14624346753	98349936	99.06	31.58
VI002872BG	38.5	95386498	14051534759	94675667	99.25	30.34

VI002934AG	38.6	100956428	14842385806	100172814	99.22	32.05
VI002986AG	38.1	110264536	16338853680	109309431	99.13	35.28
VI003057BG	38.7	105522924	15542296441	104814382	99.33	33.56
VI003135B-BL	38.5	94387268	14047038329	93390608	98.94	30.33
VI003255AG	37.8	99055188	14755125143	97726020	98.66	31.86
VI003337BG	38.7	89894206	13255609595	89094914	99.11	28.62
VI003456AG	38.8	106278456	15679639468	105088651	98.88	33.86
VI003465BG	38.4	115632864	16997323784	114587126	99.10	36.70
VI003480BG	38.2	100627792	14956434651	99782886	99.16	32.30
VI003534BG	38.3	108905074	16172568035	106698088	97.97	34.92
VI003699B-BR	38.7	103393636	15254347310	102441163	99.08	32.94
VI003894B-BLM	38.2	94378774	14002556256	93400898	98.96	30.24
VI003925B-BLM	38.7	98579442	14534665858	97866584	99.28	31.39
VI003948B-BR	38.8	110602470	16320394085	109674951	99.16	35.24
VI004069BG	38.2	108221038	16097887913	106939499	98.82	34.76
VI004184AG	38.1	111065672	16500464023	110042604	99.08	35.63
VI004243B-BR	38.3	97858906	14538755397	97146535	99.27	31.40

VI004244B-BR	38.3	117199772	17404677979	116163988	99.12	37.58
VI004312AG	38.7	94910852	14001885094	94193537	99.24	30.24
VI004432B-BR	38.7	94641712	13970450807	93998848	99.32	30.17
VI004666AG	38.8	98028200	14463568142	97255573	99.21	31.23
VI004853BG	38.6	115299028	17005975646	114380607	99.20	36.72
VI004956AG	37.9	108132250	16071655376	107196827	99.13	34.71
VI004965BG	38.1	109098962	16219658117	108270161	99.24	35.03
VI004973B-BLM	38.3	115857178	17193286881	115048196	99.30	37.13
VI005022BG	38	116969410	17418599262	115808887	99.01	37.61
VI005030BY	38.1	90933136	13520558513	88335353	97.14	29.20
VI005041AG	38.6	117271888	17308635737	115911704	98.84	37.38
VI014178BG	38.2	121729992	18099953464	120803779	99.24	39.09
VI064196	38.5	102168058	15189855794	101020176	98.88	32.80
VI064197	38.4	99581820	14825078697	98852502	99.27	32.01
BCP_075	38.7	64824598	9723689700	63537223	98.01	21.00
BCP_094	38.6	64589664	9688449600	62820738	97.26	20.92
CPI_106935	38.7	61166356	9174953400	59681199	97.57	19.81

CPI_107220	38.5	67033788	10055068200	65024377	97.00	21.71
CQ_1971	40	71679290	10751893500	71057178	99.13	23.22
CQ_2225	38.6	71861326	10779198900	70765501	98.48	23.28
CQ_2226	38.9	60240702	9036105300	56521676	93.83	19.51
CQ_2227	38.8	62187366	9328104900	60896815	97.92	20.14
CQ_2234	38.3	72144358	10821653700	69167055	95.87	23.37
CQ_2238	38.2	60553920	9083088000	56171606	92.76	19.61
CQ_2244	38.6	68888586	10333287900	51527945	74.80	22.31
CQ_2326	38.7	71213930	10682089500	70093515	98.43	23.07
CQ_2649	38.3	55374758	8306213700	53865466	97.27	17.94
CQ_2650	38.7	63250020	9487503000	61571908	97.35	20.49
CQ_2651	38.7	72644490	10896673500	66170123	91.09	23.53
CQ_2733	39.7	67389924	10108488600	66669731	98.93	21.83
CQ_2915	38.5	59197868	8879680200	58028518	98.02	19.18
CQ_2926	38.7	67832232	10174834800	67026527	98.81	21.97
CQ_3066	38.9	69412548	10411882200	68031185	98.01	22.48
CQ_3082	38.6	77342370	11601355500	76306064	98.66	25.05

CQ_3086	38.7	72397190	10859578500	70795813	97.79	23.45
CQ_3114	38.6	76035000	11405250000	74647437	98.18	24.63
CQ_3233	38.5	69654562	10448184300	68619068	98.51	22.56
CQ_3243	39	58875304	8831295600	57996075	98.51	19.07
CQ_3267	38.8	69606166	10440924900	67877694	97.52	22.55
CQ_3269	38.6	63373196	9505979400	61641160	97.27	20.53
CQ_3283	38.2	60634948	9095242200	55522294	91.57	19.64
CQ_3293	38.3	70636224	10595433600	68981512	97.66	22.88
CQ_3323	38.6	69759192	10463878800	68547136	98.26	22.60
Karumbyar	38.6	213776592	31222432351	211497414	98.93	67.42
NAM28	38.2	192620538	28006223559	190160711	98.72	60.48
NAM29	38.4	187196374	27210646221	184919246	98.78	58.76
NAM30	38.6	174386998	25414019497	172453908	98.89	54.88
TPI_25	39	66252234	9937835100	65532983	98.91	21.46
VI032155	38.2	104377702	15536268464	103054321	98.73	33.55
VI032156	38.3	108713520	16186446077	107553969	98.93	34.95
VI035226	38.3	97733110	14546845659	92007079	94.14	31.41

Supplementary Table S2. List of accessions used in this study

Accession	Taxonomy	Country of collection	Genetic group
Crystal	*Vigna radiata* var. *radiata*	Unknown	Admixed_Rad
NAM1	*Vigna radiata* var. *radiata*	Philippines	RadOther
NAM2	*Vigna radiata* var. *radiata*	Unknown	RadOther
NAM3	*Vigna radiata* var. *radiata*	Unknown	Admixed_Rad
NAM4	*Vigna radiata* var. *radiata*	Unknown	Admixed_Rad
NAM5	*Vigna radiata* var. *radiata*	Unknown	RadOther
NAM6	*Vigna radiata* var. *radiata*	Unknown	RadOther
NAM7	*Vigna radiata* var. *radiata*	Unknown	Admixed_Rad
NAM8	*Vigna radiata* var. *radiata*	Unknown	Admixed_Rad
NAM9	*Vigna radiata* var. *radiata*	India	RadSA
NAM10	*Vigna radiata* var. *radiata*	Unknown	RadSA
NAM11	*Vigna radiata* var. *radiata*	Unknown	RadOther
NAM12	*Vigna radiata* var. *radiata*	Unknown	RadOther
NAM13	*Vigna radiata* var. *radiata*	Unknown	RadOther
NAM15	*Vigna radiata* var. *radiata*	Unknown	RadOther
NAM16	*Vigna radiata* var. *radiata*	Unknown	RadSA
NAM17	*Vigna radiata* var. *radiata*	Unknown	RadSA
NAM18	*Vigna radiata* var. *radiata*	Unknown	RadOther
NAM19	*Vigna radiata* var. *radiata*	Unknown	RadOther
NAM20	*Vigna radiata* var. *radiata*	Taiwan	Admixed_Rad
NAM21	*Vigna radiata* var. *radiata*	Unknown	Admixed_Rad
NAM22	*Vigna radiata* var. *radiata*	Unknown	RadOther
NAM23	*Vigna radiata* var. *radiata*	Pakistan	RadSA

NAM24	*Vigna radiata* var. *radiata*	India	RadSA
NAM26	*Vigna radiata* var. *radiata*	Unknown	Admixed_Rad
NAM27	*Vigna radiata* var. *radiata*	Unknown	RadOther
VI000020AY	*Vigna radiata* var. *radiata*	Thailand	RadOther
VI000099AG	*Vigna radiata* var. *radiata*	India	Admixed_Rad
VI000232AG	*Vigna radiata* var. *radiata*	Iran	RadOther
VI000238AG	*Vigna radiata* var. *radiata*	Afghanistan	RadOther
VI000542BY	*Vigna radiata* var. *radiata*	India	RadSA
VI000578AG	*Vigna radiata* var. *radiata*	India	RadSA
VI000625B-BR	*Vigna radiata* var. *radiata*	India	RadOther
VI000938AG	*Vigna radiata* var. *radiata*	India	RadSA
VI001191BG	*Vigna radiata* var. *radiata*	Philippines	RadOther
VI001435AG	*Vigna radiata* var. *radiata*	USA	RadSA
VI001509AG	*Vigna radiata* var. *radiata*	Pakistan	RadOther
VI001514AG	*Vigna radiata* var. *radiata*	India	RadSA
VI001728AG	*Vigna radiata* var. *radiata*	India	RadSA
VI001806BG	*Vigna radiata* var. *radiata*	Pakistan	Admixed_Rad
VI002176BG	*Vigna radiata* var. *radiata*	India	Admixed_Rad
VI002197BG	*Vigna radiata* var. *radiata*	Korea	RadOther
VI002239AG	*Vigna radiata* var. *radiata*	Afghanistan	RadOther
VI002456AG	*Vigna radiata* var. *radiata*	Korea	RadOther
VI002647AG	*Vigna radiata* var. *radiata*	Thailand	RadOther
VI002859BG	*Vigna radiata* var. *radiata*	Iran	RadOther
VI002872BG	*Vigna radiata* var. *radiata*	Iran	Admixed_Rad
VI002934AG	*Vigna radiata* var. *radiata*	India	Admixed_Rad

VI002986AG	*Vigna radiata* var. *radiata*	India	RadSA
VI003057BG	*Vigna radiata* var. *radiata*	India	Admixed_Rad
VI003135B-BL	*Vigna radiata* var. *radiata*	India	Admixed_Rad
VI003255AG	*Vigna radiata* var. *radiata*	India	Admixed_Rad
VI003337BG	*Vigna radiata* var. *radiata*	India	RadSA
VI003456AG	*Vigna radiata* var. *radiata*	Unknown	RadSA
VI003465BG	*Vigna radiata* var. *radiata*	India	RadSA
VI003480BG	*Vigna radiata* var. *radiata*	India	Admixed_Rad
VI003534BG	*Vigna radiata* var. *radiata*	India	RadSA
VI003699B-BR	*Vigna radiata* var. *radiata*	India	RadSA
VI003894B-BLM	*Vigna radiata* var. *radiata*	India	RadSA
VI003925B-BLM	*Vigna radiata* var. *radiata*	India	RadSA
VI003948B-BR	*Vigna radiata* var. *radiata*	India	RadOther
VI004069BG	*Vigna radiata* var. *radiata*	India	Admixed_Rad
VI004184AG	*Vigna radiata* var. *radiata*	Netherlands	RadOther
VI004243B-BR	*Vigna radiata* var. *radiata*	Turkey	RadOther
VI004244B-BR	*Vigna radiata* var. *radiata*	India	RadOther
VI004312AG	*Vigna radiata* var. *radiata*	India	RadOther
VI004432B-BR	*Vigna radiata* var. *radiata*	Iran	RadOther
VI004666AG	*Vigna radiata* var. *radiata*	Iran	RadOther
VI004853BG	*Vigna radiata* var. *radiata*	India	Admixed_Rad
VI004956AG	*Vigna radiata* var. *radiata*	Pakistan	RadSA
VI004965BG	*Vigna radiata* var. *radiata*	Pakistan	Admixed_Rad
VI004973B-BLM	*Vigna radiata* var. *radiata*	India	RadSA
VI005022BG	*Vigna radiata* var. *radiata*	India	RadSA

VI005030BY	*Vigna radiata* var. *radiata*	Mexico	RadOther
VI005041AG	*Vigna radiata* var. *radiata*	Unknown	RadOther
VI014178BG	*Vigna radiata* var. *radiata*	Kenya	RadOther
VI064196	*Vigna radiata* var. *radiata*	Myanmar	Admixed_Rad
VI064197	*Vigna radiata* var. *radiata*	Myanmar	RadSA
BCP_075	*Vigna radiata* var. *sublobata*	Papua New Guinea	SubAUe
BCP_094	*Vigna radiata* var. *sublobata*	Papua New Guinea	SubAUw
CPI_106935	*Vigna radiata* var. *sublobata*	Indonesia	SubTI
CPI_107220	*Vigna radiata* var. *sublobata*	Indonesia	SubAUe
CQ_1971	*Vigna radiata* var. *sublobata*	Australia	SubAUe
CQ_2225	*Vigna radiata* var. *sublobata*	Australia	SubAUe
CQ_2226	*Vigna radiata* var. *sublobata*	Australia	SubAUe
CQ_2227	*Vigna radiata* var. *sublobata*	Australia	SubAUe
CQ_2234	*Vigna radiata* var. *sublobata*	Australia	SubAUe
CQ_2238	*Vigna radiata* var. *sublobata*	Australia	SubAUe
CQ_2244	*Vigna radiata* var. *sublobata*	Australia	SubAUw
CQ_2326	*Vigna radiata* var. *sublobata*	Australia	SubAUe
CQ_2649	*Vigna radiata* var. *sublobata*	Australia	SubAUw
CQ_2650	*Vigna radiata* var. *sublobata*	Australia	SubAUe
CQ_2651	*Vigna radiata* var. *sublobata*	Australia	SubAUe
CQ_2733	*Vigna radiata* var. *sublobata*	Australia	SubAUe
CQ_2915	*Vigna radiata* var. *sublobata*	Australia	SubAUe
CQ_2926	*Vigna radiata* var. *sublobata*	Australia	SubAUw
CQ_3066	*Vigna radiata* var. *sublobata*	Australia	SubAUe
CQ_3082	*Vigna radiata* var. *sublobata*	Australia	SubAUw

CQ_3086	*Vigna radiata* var. *sublobata*	Australia	SubAUw
CQ_3114	*Vigna radiata* var. *sublobata*	Australia	SubAUe
CQ_3233	*Vigna radiata* var. *sublobata*	Australia	SubAUw
CQ_3243	*Vigna radiata* var. *sublobata*	Australia	SubAUw
CQ_3267	*Vigna radiata* var. *sublobata*	Australia	SubAUw
CQ_3269	*Vigna radiata* var. *sublobata*	Australia	SubAUw
CQ_3283	*Vigna radiata* var. *sublobata*	Australia	SubAUe
CQ_3293	*Vigna radiata* var. *sublobata*	Australia	SubAUw
CQ_3323	*Vigna radiata* var. *sublobata*	Australia	SubAUe
Karumbyar	*Vigna radiata* var. *sublobata*	India	SubAS
NAM28	*Vigna radiata* var. *sublobata*	Australia	SubAUe
NAM29	*Vigna radiata* var. *sublobata*	Australia	SubAUe
NAM30	*Vigna radiata* var. *sublobata*	Indonesia	SubTI
TPI_25	*Vigna radiata* var. *sublobata*	Australia	SubAUe
VI032155	*Vigna radiata* var. *sublobata*	Australia	SubAUe
VI032156	*Vigna radiata* var. *sublobata*	Madagascar	SubAS
VI035226	*Vigna mungo*	Australia	Outgroup

0

Supplementary Table S3. Measurement of seed weight in wild accessions from genetic groups of SubAU and SubAS. The data are presented as mean ± standard error.

Accession	Genetic group	Seed weight (mg/100 seeds)	Seed number (seeds/pod)	Pod length (cm)
CQ2234	SubAU	1491.82 ± 39.18	7.83 ± 0.2	4.06 ± 0.06
NAM30	SubAU	1198.19 ± 63.64	9.63 ± 0.27	3.74 ± 0.06
CQ3267	SubAU	1808.12 ± 58.44	7.87 ± 0.33	4.54 ± 0.12
Karumbyar	SubAS	2775.46 ± 106.63	11.87 ± 0.23	5.63 ± 0.08
VI032156	SubAS	2176.56 ± 209.72	9.53 ± 0.32	5.47 ± 0.09

Supplementary Table S4. List of GPS sites of wild mungbeans used for niche modeling

Region	Longitude	Latitude	Source
South Asia	71.397	25.752	NBPGR
South Asia	73.312	28.023	NBPGR
South Asia	73.312	16.99	NBPGR
South Asia	73.383	18.75	NBPGR
South Asia	73.559	21.876	NBPGR
South Asia	75.303	22.601	NBPGR
South Asia	76.071	11.051	NBPGR
South Asia	76.214	10.528	NBPGR
South Asia	76.655	10.787	NBPGR
South Asia	76.956	11.017	NBPGR
South Asia	77.103	9.919	NBPGR
South Asia	77.167	19.817	GBIF
South Asia	78.767	15.417	GBIF
South Asia	78.883	12.867	GBIF
South Asia	79.017	11.417	AGG
South Asia	79.017	11.433	GBIF
South Asia	79.986	23.182	NBPGR
South Asia	80.017	17.817	GBIF
South Asia	80.067	23.067	GBIF
South Asia	80.167	17.55	GBIF
South Asia	81.067	17.717	GBIF
South Asia	81.883	18.344	NBPGR

Southeast Asia	100.673	-0.322	GBIF
Southeast Asia	107.009	-6.741	GBIF
Southeast Asia	106.791	-6.59	GBIF
Southeast Asia	107.005	-6.738	GBIF
Southeast Asia	107.621	-6.913	GBIF
Southeast Asia	108.211	-7.654	GBIF
Southeast Asia	109.923	-7.187	GBIF
Southeast Asia	114.133	-8.083	GBIF
Southeast Asia	106.978	-6.703	GBIF
Southeast Asia	120.338	23.235	GBIF
Southeast Asia	121.514	22.056	GBIF
Southeast Asia	120.822	24.253	GBIF
Southeast Asia	120.848	21.903	GBIF
Southeast Asia	121.53	25.008	GBIF
Southeast Asia	120.871	24.271	GBIF
Southeast Asia	120.202	22.989	GBIF
Southeast Asia	120.669	22.344	GBIF
Southeast Asia	120.282	22.628	GBIF
Southeast Asia	120.321	22.823	GBIF
Southeast Asia	98.7	19.117	GBIF
Southeast Asia	98.733	19.2	GBIF
Southeast Asia	98.783	18.95	GBIF
Southeast Asia	99.217	18.333	GBIF
Southeast Asia	99.833	20.3	GBIF
Southeast Asia	99.867	18.333	GBIF

Southeast Asia	101.063	13.254	GBIF
Southern Hemisphere	120.167	-1.167	AGG
Southern Hemisphere	152.55	-27.117	AGG
Southern Hemisphere	152.583	-26.517	AGG
Southern Hemisphere	148.167	-23.667	AGG
Southern Hemisphere	148.15	-22.233	AGG
Southern Hemisphere	149.25	-21.5	AGG
Southern Hemisphere	148.383	-21.133	AGG
Southern Hemisphere	119.667	-20.833	AGG
Southern Hemisphere	144.3	-18.667	AGG
Southern Hemisphere	146.165	-18.581	AGG
Southern Hemisphere	125.383	-18.083	AGG
Southern Hemisphere	127.8	-18.033	AGG
Southern Hemisphere	122.253	-17.781	AGG
Southern Hemisphere	122.209	-17.706	AGG
Southern Hemisphere	145.5	-17.017	AGG
Southern Hemisphere	129.151	-16.866	AGG
Southern Hemisphere	125.933	-16.717	AGG
Southern Hemisphere	131.2	-16.367	AGG
Southern Hemisphere	133.05	-16.217	AGG
Southern Hemisphere	130.383	-15.633	AGG
Southern Hemisphere	145.25	-15.483	AGG
Southern Hemisphere	128.117	-15.467	AGG
Southern Hemisphere	131.733	-15.067	AGG
Southern Hemisphere	131.183	-13.833	AGG

Southern Hemisphere	132.32	-12.554	AGG
Southern Hemisphere	131.05	-12.533	AGG
Southern Hemisphere	136.883	-12.25	AGG
Southern Hemisphere	123.633	-10.217	AGG
Southern Hemisphere	123.567	-10.167	AGG
Southern Hemisphere	124.167	-10	AGG
Southern Hemisphere	124.567	-9.517	AGG
Southern Hemisphere	124.5	-9.483	AGG
Southern Hemisphere	124.77	-9.45	AGG
Southern Hemisphere	143.42	-9.007	AGG
Southern Hemisphere	126.3	-7.7	AGG
Southern Hemisphere	134.333	-6.75	AGG
Southern Hemisphere	146.997	-6.738	AGG
Southern Hemisphere	146.717	-6.583	AGG
Southern Hemisphere	144.933	-4.267	AGG

4

5

Supplementary Table S5. List of primers used in this study

Primer	Sequence	Target gene
Vrdet1-P3-F	GGCAAGAATGCCTTTGGAACC	*VrDet1*
Vrdet1-P3-R	AGCATCTGTTGTGCCTGGAA	*VrDet1*
VrMYB26-qPCR-F2	GGTTGCTGGAGTTCCGTCCCAAAA	*VrMYB26a*
VrMYB26-qPCR-R	AACCATTGGCAAGACCGTGA	*VrMYB26a*
CYP20-F	TCCCCAAACAGCCGAAAA	*VrCYP20*
CYP20-R	CCCCTTGAATCATGAAATCCTT	*VrCYP20*
VrCAD4-cDNA-F2	CCTACAATCTAAGAAACACTGGCCCTGATG	*VrCAD4*
VrCAD4-cDNA-R2	AACTACCTCGTGTCCGGGGA	*VrCAD4*